Technical Report

TR-01-02

Borehole radar and BIPS investigations in boreholes at the Boda area

Seje Carlsten, Allan Stråhle
GEOSIGMA AB

December 2000

Svensk Kärnbränslehantering AB
Swedish Nuclear Fuel
and Waste Management Co
Box 5864
SE-102 40 Stockholm Sweden
Tel 08-459 84 00
+46 8 459 84 00
Fax 08-661 57 19
+46 8 661 57 19

Borehole radar and BIPS investigations in boreholes at the Boda area

Seje Carlsten, Allan Stråhle
GEOSIGMA AB

December 2000

Keywords: Boda, caves, borehole radar, BIPS, deviation measurements.

Abstract

As part of the studies conducted in the Boda area, measurements with borehole radar, borehole TV (BIPS) and deviation measurements were performed during May 2000. The investigations were carried out in four percussion-drilled boreholes with a total length of 514 m. Two boreholes are vertical and two are directed into and below the cave area.

The BIPS measurement showed the presence of 14 open fractures. Largest apparent aperture width of open fractures was 133 mm. In the lowest part in boreholes 2, 3, and 4, particles in suspension deteriorated the visibility. BIPS has revealed a dominating subhorizontal fracture set and another striking NW to N-S with a dip close to vertical. Possible but very uncertain is a third fracture set striking NE and dipping steeply towards S. The open and partly open fractures forms an average blocksize 11 m wide and 6 m high, while the length of the block is uncertain.

Of 98 borehole radar reflectors interpreted to intersect within BIPS-mapped sections, 90 were possible to combine with BIPS-mapped structures, i.e. 92% of the radar reflectors.

The fractured rock around Boda is a shallow feature, since borehole radar and BIPS measurements shows no evidence of increased fracturing or the presence of caves at larger depth in the Boda area. The result indicates that the formation of the superficial fracture system (with caves included) at Boda in all probability is connected to glacial action, such as banking.

Sammanfattning

Som en del av utförda undersökningar i Bodaområdet, har mätningar med borrhålsradar, borrhåls-TV (BIPS) och borrhålsdeviation utförts under maj 2000. Undersökningarna genomfördes i fyra hammarborrade hål med en sammanlagd längd av 514 m. Två av borrhålen är vertikala medan två är riktade in mot och under själva grottområdet.

BIPS mätningarna påvisade 14 öppna sprickor. Störst skenbar apertur på öppen spricka var 133 mm. I den nedersta delen i borrhål 2, 3 och 4 försämrades sikten genom partiklar i borrhålsvätskan. BIPS visar på en dominerande subhorisontell sprickbildning samt en NV-N strykande subvertikal. En tredje, mer osäker sprickriktning stryker i NO med en brant stupning. De öppna och delvis öppna sprickorna bildar block som är i medeltal 11 m breda och 6 m höga medan deras längd är osäker.

Av 98 tolkade radarreflexer kunde 90 kombineras ihop med strukturer från BIPS-karteringen, dvs 92% av radarreflexerna.

Det spruckna berget med enskilda grottor är ett ytligt fenomen, eftersom varken borrhålsradar eller BIPS har påvisat förekomst av grottor på större djup i Bodaområdet. Resultatet indikerar att bildningen av det ytliga spricksystemet (med grottor) med all sannolikhet är sammankopplat med glacial påverkan såsom bankning.

Contents

1 Introduction

At Boda, a system of caves in the crystalline bedrock has been discovered and mapped. An investigation regarding the cause and vertical extent of the caves commenced late 1997 and was reported in April 2000 (Wänstedt, 2000).

This report present the continued investigations performed during late spring 2000 by GEOSIGMA AB in the Boda area, close to and east of Iggesund in Hudiksvall's municipality, at the eastern coast of Sweden, Figure 1-1. A geological map of the area is presented in Figure 1-2. The investigations comprise borehole radar, borehole TV (BIPS), and borehole deviation measurements.

1.1 Objective

The objective of the borehole radar and BIPS investigations presented in this report is to determine the vertical extent of the fracturing and to acquire possible information about the presence of caves at depth in the area.

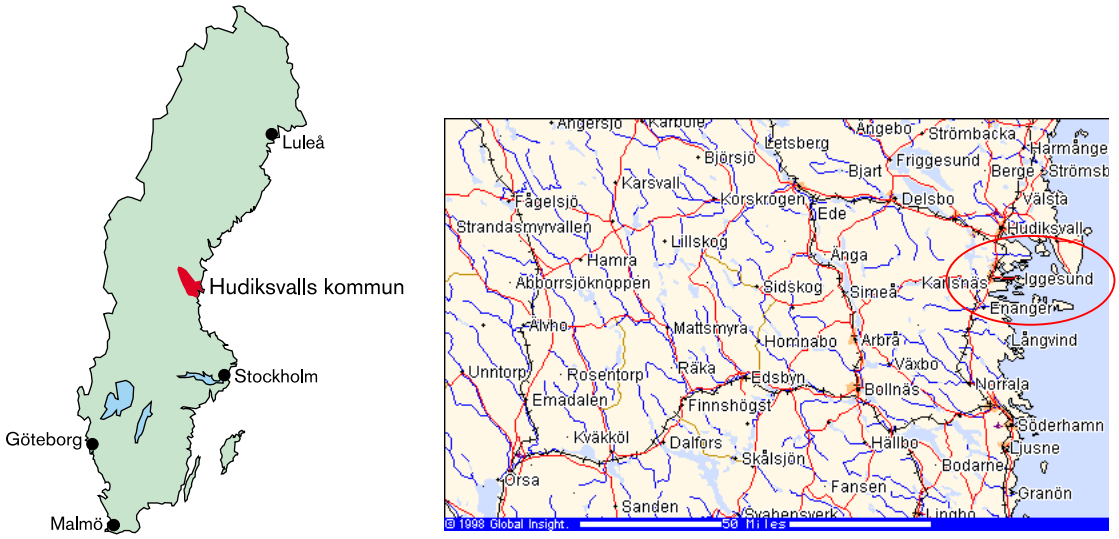

Figure 1-1. Location of Hudiksvall municipality (left) and Iggesund (right).

GEOLOGIC MAP OF THE AREA SURROUNDING THE BODA CAVES.

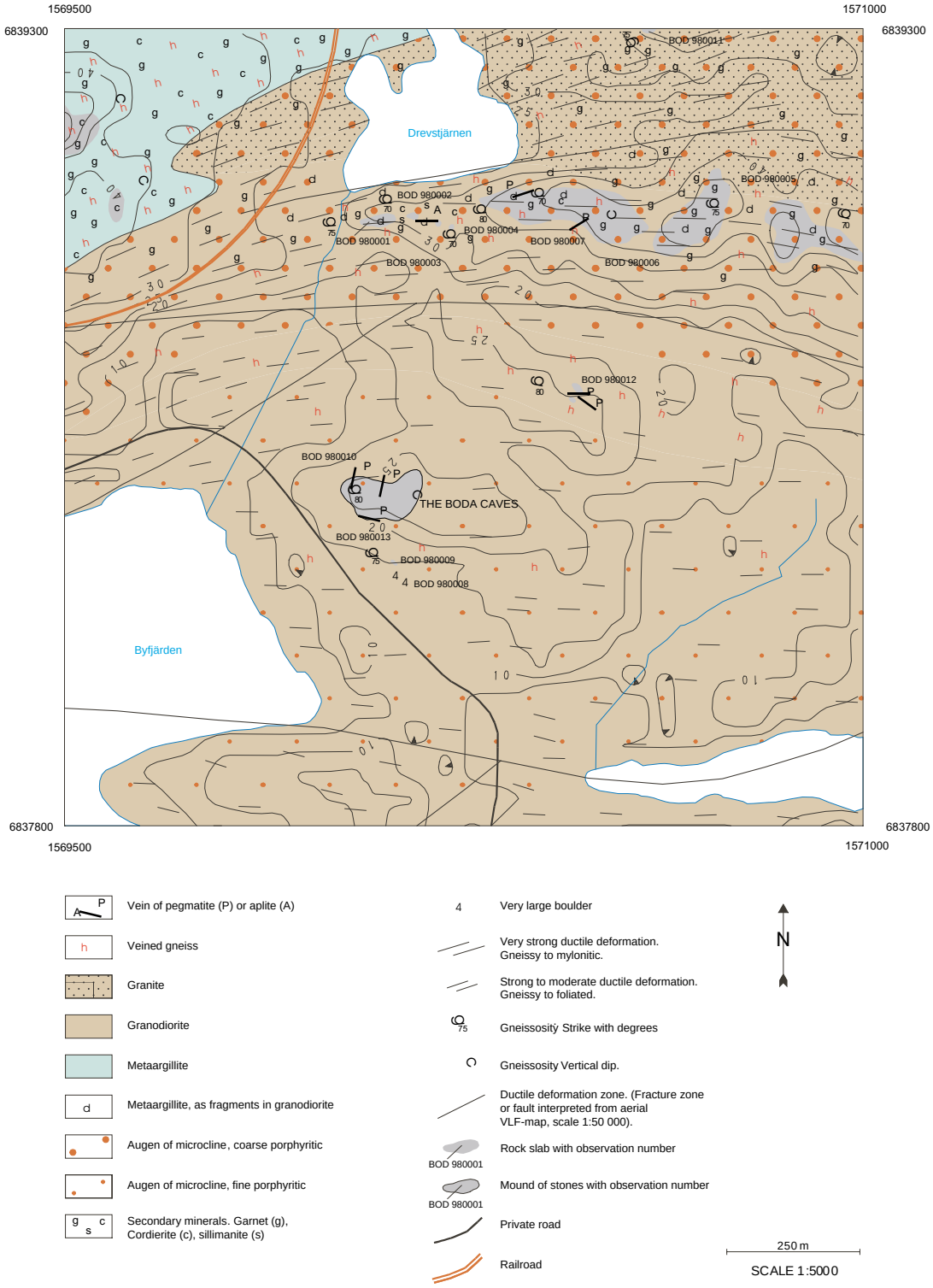

Figure 1-2. Geological map of the Boda area and its surroundings (Wänstedt, 2000).

2 Borehole location

Deviation measurements were performed in the four percussion-drilled boreholes. Data from the measurements is presented in Appendix 1. Table 2-1 is an overview of calculated mean values from the deviation data. A map with location of the boreholes is found in Figure 2-1, while Figures 2-2 to 2-5 shows pictures in field of the boreholes at the site.

Borehole 1 was drilled vertically and located close to the dipping borehole 2. The purpose of borehole 1 was, together with borehole 2, to cover a large rock volume in order to trace the presence of open fractures or caves at larger depths. The dipping borehole 3 was drilled from the new parking lot and directed towards east. The purpose of this borehole was similar to that of borehole 2, i.e. to penetrate the rock mass below the cave area and to drill in a slightly different direction than borehole 2. The vertical borehole 4 was drilled from a location northwest of the cave area, with the purpose to investigate the rock mass on this side of the cave area.

Table 2-1. Borehole data for percussion drilled holes in the Boda area. Inclination and declination values are calculated from deviation measurements.

Borehole	Length	Inclination	Declination	Z* m.a.s.l.
1	100	87.6	184	11.5
2	184	50.2	40	11.5
3	130	41.3	90	14.5
4	100	85.7	64	13.5

* Estimated value

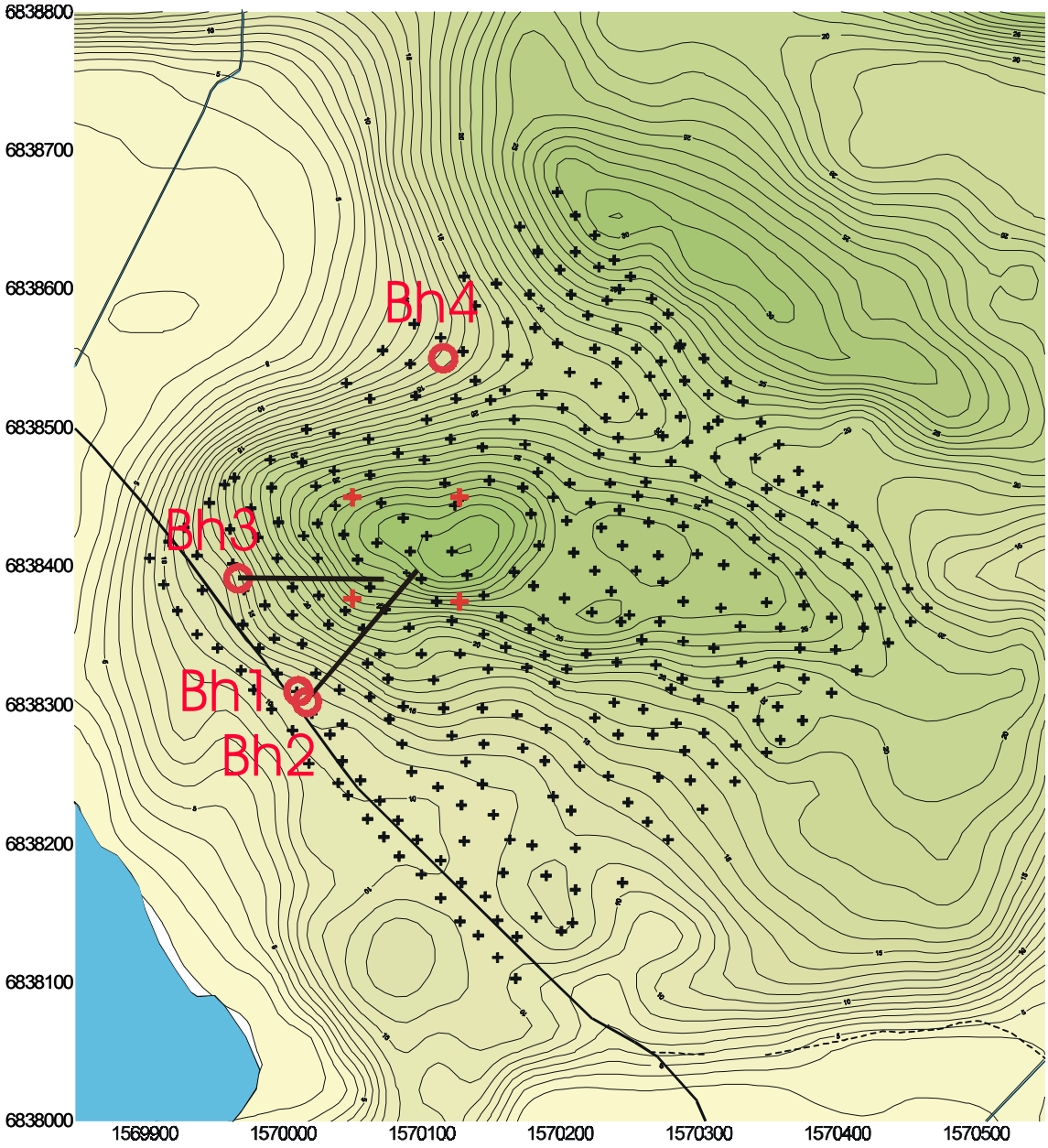

Figure 2-1. Close-up of the area showing the topography, the coordinates of the area surrounding the cave, and a square (red crosses) approximately outlining the cave area. The actual cave area is about 150 x 150 m. Red circles indicate location of boreholes.

Figure 2-2. The vertical borehole 1 at the Boda site. The BIPS probe is lowered into the borehole. Please note the centralizers on the probe.

Figure 2-3. The vertical borehole 1 (to the left) and the dipping borehole 2 (to the right) at the old parking lot. Borehole 2 is directed into and under the cave area.

Figure 2-4. The dipping borehole 3 located in the ditch at the new parking lot at Boda. The borehole is directed into and under the cave area.

Figure 2-5. Overview of the vertical borehole 4 located northwest of the cave area. Observe the dead cow scull to the right in the picture.

3 Methods

3.1 Borehole radar measurements

Borehole radar measurements using dipole antennas with 100 MHz and 250 MHz have been performed in the percussion-drilled boreholes 1–4. A general description of the RAMAC-system and the interpretation of data are given by Sandberg et al. (1991).

Due to the dimension of the borehole (115 mm) compared to the dimension of the radar probe (48 mm), it was found necessary to use plastic centralizers in order to keep the probe in the centre of the borehole.

Measurements with 100 MHz have been the basis for the interpretation and presentation of radar data due to the better quality of these data compared to the data from 250 MHz. The large borehole diameter caused a strong ringing of the 250 MHz radar pulse that disturbs the quality of the radar map. Radar pulses reflected from the borehole wall cause the ringing which shows as parallel bands in the raw data. The parallel bands obscure relevant radar reflectors.

3.1.1 Short description of the radar method

The RAMAC-system (Figure 3-1), used in this project, is a short pulse radar system, i.e. the length of the emitted EM pulse is in the order of a wavelength. The system is built for field use. The acquisition procedure is efficient and can be carried out by a one person. Figure 3-1 shows the main parts of the equipment. During operation, a short electromagnetic pulse is transmitted into the rock surrounding the borehole. A receiver antenna, similar to the transmitter antenna, picks up the incoming signal, amplifies it and records its strength as a function of time. The receiver is normally placed in the same borehole as the transmitter, but can be placed in another borehole or on ground surface, if desired. The distance (travel-time) to a reflector, the strength of the reflection and the attenuation of the direct wave, travelling along the borehole wall from the transmitter to the receiver, can be recorded. The principles of radar measurements are shown in Figure 3-2.

Figure 3-1. Picture of main parts of the RAMAC/GPR borehole radar system. Transmitter and receiver antennas in the front, control unit to the left, and measuring wheel to the right. Large box in the middle is the transport box.

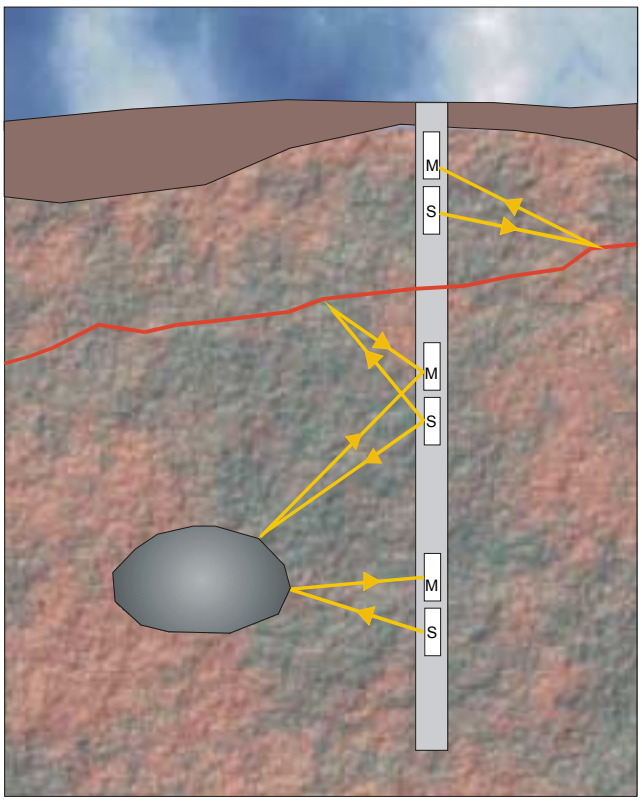

Figure 3-2. Principles of borehole radar measurement. The figure shows different positions of the transmitter (S) and receiver (M) antennas in the same borehole and examples of reflectors.

3.1.2 Operation procedure

The transmitter and the receiver are connected to each other at a fixed distance. A cable is connected to the upper part of the probe arrangement and the probe is lowered into the borehole. Measurements are performed about each 0.1 meter during downward and continuous movement of the probe to the bottom of the borehole.

The upper part of the probe is levelled to the top of casing. A digitally measuring wheel on which the fibre optic cable runs records length. The cable is connected to the control box and the computer that masters the different values controlling the radar measurement.

Details of the measurements are given in Table 3-1.

3.1.3 Processing of data

When the interpretation software reads raw data, the variation in DC-current is removed simultaneously. The first step of processing involves finding the zero time or the arrival time of the airwave pulse travelling in the borehole. Applying different type of gains and filters made further enhancement of the signals. Once filtered, the distance from borehole axis is converted from time to depth. The velocity of radar waves was chosen to 120 m/ms.

3.1.4 Presentation of data

Processed radar data from each borehole is presented in a separate figure for each borehole. The borehole length is shown on the vertical axis and the distance from borehole on the horizontal axis. Interpretation of the radar maps is presented in separate figures and in tables. All interpreted borehole lengths refers to the top of casing (TOC) for each individual borehole.

Table 3-1. Specifications of borehole radar measurements in boreholes 1–4.

General for 100 MHz	
Type of measurement:	Dipole antenna, singlehole reflection mode.
Centre frequency:	100 MHz
Transmitter-receiver separation:	2.75 m
Sampling frequency:	745.370 MHz
No. of samples:	512
No. of stackings:	16
Borehole 1	
Adjusted measurement length:	2.05–94.69 m
Depth increment:	0.092 m
No. of records:	1007
Date of measurement:	000522
Borehole 2	
Adjusted measurement length:	2.05–181.82 m
Depth increment:	0.092 m
No. of records:	1954
Date of measurement:	000522
Borehole 3	
Adjusted measurement length:	2.05–128.64 m
Depth increment:	0.092 m
No. of records:	1376
Date of measurement:	000523
Borehole 4	
Adjusted measurement length:	2.05–94.51 m
Depth increment:	0.092 m
No. of records:	1005
Date of measurement:	000523
General for 250 MHz	
Type of measurement:	Dipole antenna, singlehole reflection mode.
Centre frequency:	250 MHz
Transmitter-receiver separation:	1.7 m
Sampling frequency:	1032.051 MHz
No. of samples:	512
No. of stackings:	16
Borehole 1	
Adjusted measurement length:	1.20–95.28 m
Depth increment:	0.096 m
No. of records:	980
Date of measurement:	000522

Borehole 2

Adjusted measurement length:	1.20–182.93 m
Depth increment:	0.096 m
No. of records:	1893
Date of measurement:	000522

Borehole 3

Adjusted measurement length:	1.20–128.02 m
Depth increment:	0.096 m
No. of records:	1321
Date of measurement:	000523

Borehole 4

Adjusted measurement length:	1.20–95.28 m
Depth increment:	0.096 m
No. of records:	980
Date of measurement:	000523

Figure 3-3. Measurement of borehole 1. The measuring wheel and the fibre optic cable can be seen in the picture.

3.1.5 Results from borehole 1

Borehole 1 was measured from 2.05 meter to 94.7 meter. The quality of the radar measurement is good and the penetration of radar waves around the borehole is up to 20 meter. A radar map from the borehole is presented in Figure 3-4 and the interpretation of the radar map is shown in Figure 3-5 and in Table 3-2.

From the radar map it can be seen that there are several reflectors (structures) that are exhibiting a strong character in the radar map, and can be traced over large distances. Examples on prominent structures in this borehole are reflector 4, 6, 23, 11, and 13.

Table 3-2. Results from radar investigation in borehole 1.

Reflector ID	Length of intersection related to TOC (m)	Angle of intersection (deg.)	Magnitude 1=weak 2=medium 3=strong U=uncert.	Comments
1	–3.1	54	2	Several parallel reflectors
2	1.2	25	3	Undulating
3	4.9	49	3	
19	6.9	90	1	
4	10.9	16	3	
5	15.6	34	2	
6	18.1	14	3	
7	22.5	25	2	
8	36.8	22	2	Undulating
9	37.7	60	2	
17	43.6	28	2	
10	54.7	46	2	
20	65.4	41	2	
23	76.4	50	3	
11	77.3	37–44	3	Difference in angle between upper and lower limb
13	81.0	17	3	
12	82.5	44	2	
18	93.4	32	2	Short
22	97.3	13	1	Undulating
14	104.3	44	2	
21	105.3	14	2	Undulating

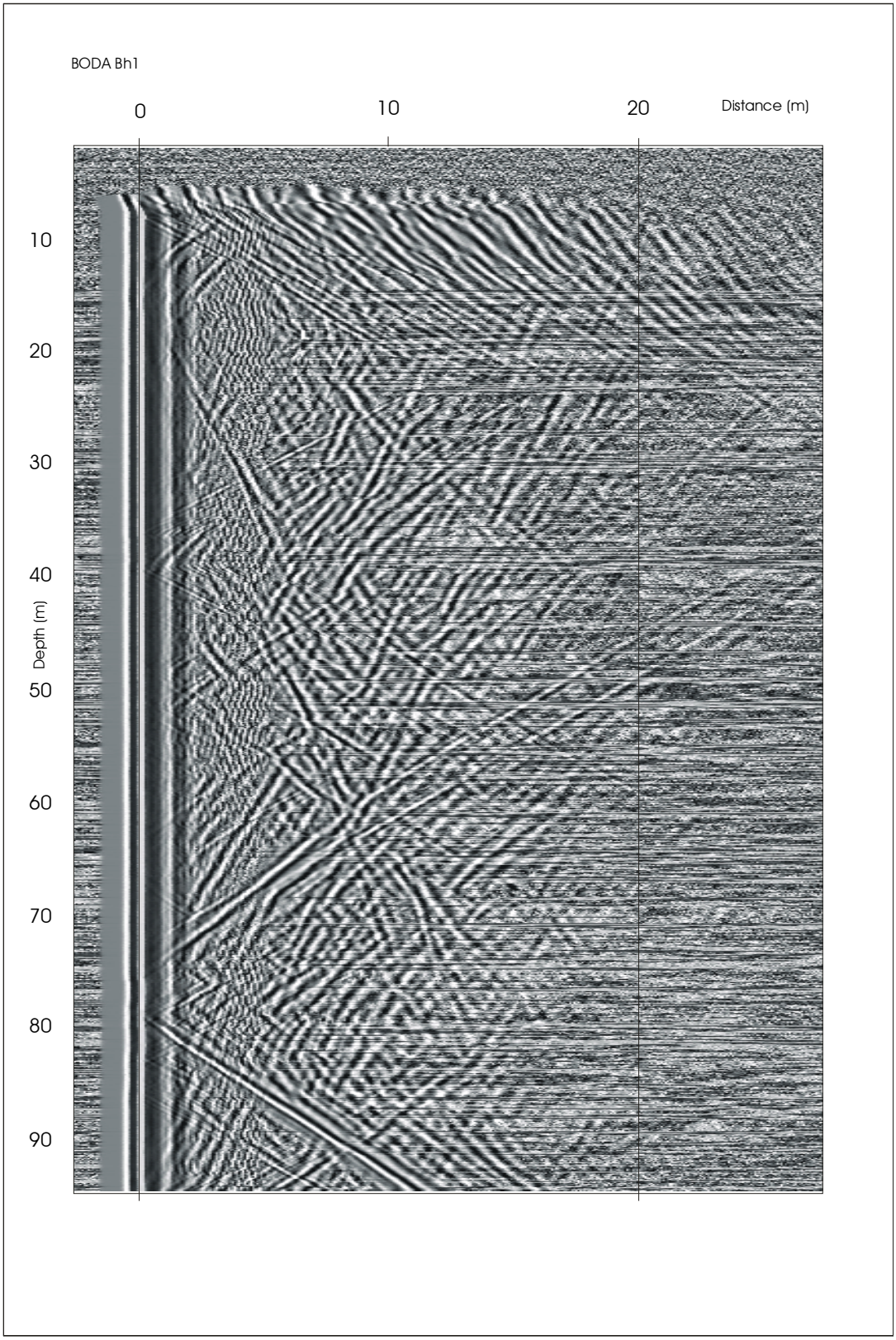

Figure 3-4. Radar reflection map from borehole 1.

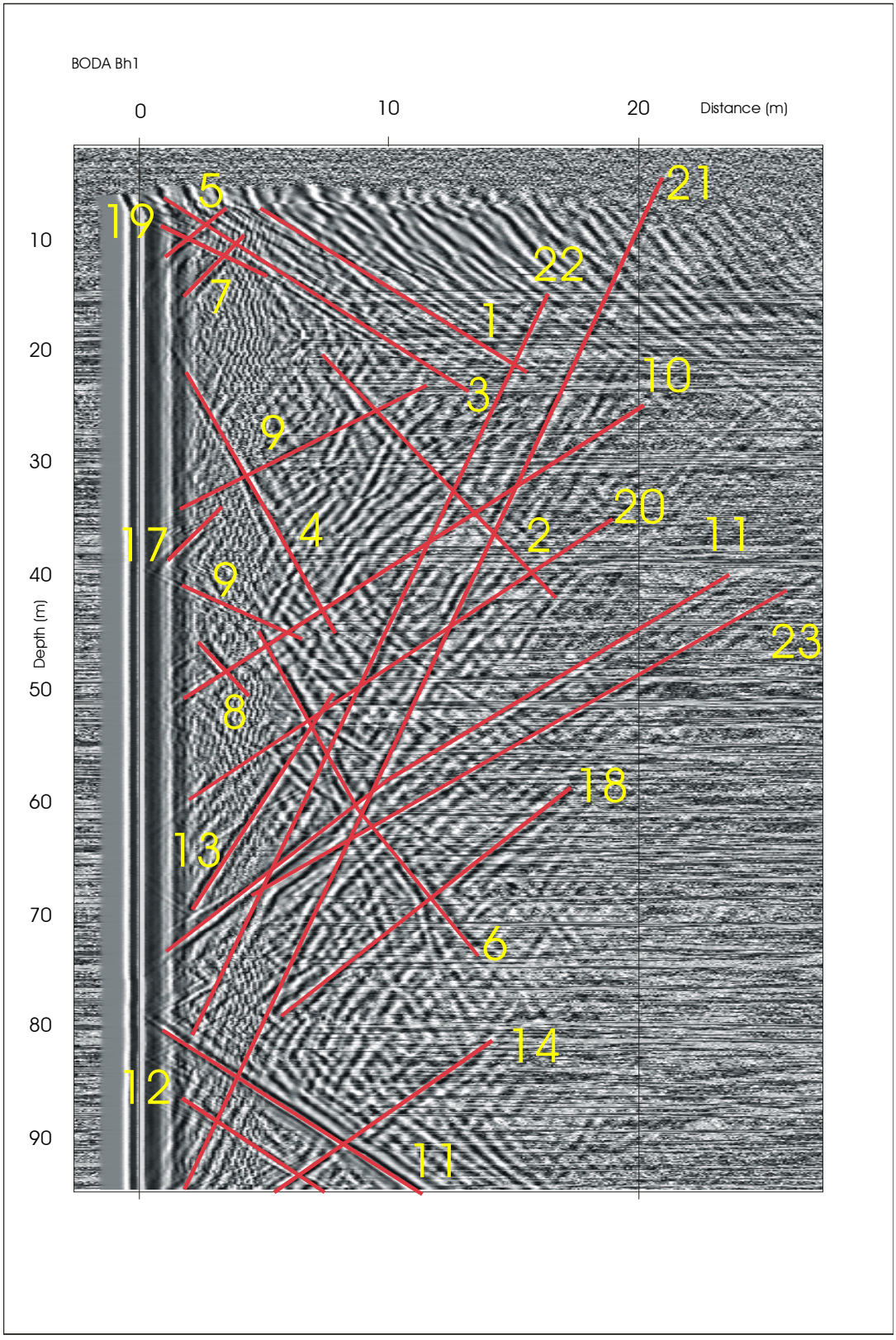

Figure 3-5. Radar interpretation map for borehole 1.

3.1.6 Results from borehole 2

The dipping borehole 2 was measured from 2.05 meter to 181.8 meter, i.e. the longest borehole at the site. The quality of the radar measurement is good and the penetration of radar waves around the borehole is up to 20 meter, and in some parts even up to 25 meter. A radar map from the borehole is presented in Figure 3-6 to 3-7 and the interpretation of the radar map is shown in Figure 3-8 to 3-9 and in Table 3-3.

Several reflectors (structures) in the radar map are showing a strong character in the radar map, and can be traced over large distances. Some reflectors cease against other reflectors. The most prominent reflectors in the radar map are reflectors 1, 2, 11, 17 and 15.

Table 3-3. Results from radar investigation in borehole 2.

Reflector ID	Length of intersection related to TOC (m)	Angle of intersection (deg.)	Magnitude 1=weak 2=medium 3=strong U=uncert.	Comments
1	5.5	47	3	
2	9.2	39	3	
3	14.4	40	2	
35	15.1	24	1	
4	22.8	40	2	Short
40	26.1	51	1	
5	26.3	31	1	
6	29.7	15	3	
39	31.0	50	1	
7	37.4	35	2	
8	39.2	51	1	
9	55.8	27	2	
10	60.8	23	3	
11	63.3	41	3	
12	71.5	42	2	
13	73.4	35	2	
14	73.9	39	3	
42	80.1	38	2	
16	82.4	19	2	
17	83.7	44	3	
15	83.9	50	2	Parallel reflectors at 82.5/51 and 85.6/49
18	90.5	35	2	Short
19	94.6	52	2	Short
41	96.8	64	1	
20	108.1	21	2	
21	110.1	49	3	
43	111.3	31	2	
23	117.2	55	2	
22	118.6	23	2	
34	119.4	35	2	Undulating
20	124.7	45	1	
24	126.5	54	2	
25	131.7	32	3	Undulating
26	134.7	22	2	
38	138.4	50	2	
37	139.6	48	2	
27	142.1	33	2	Short
28	158.8	31	2	Short
36	169.4	26	1	
29	172.8	28	1	
30	174.8	41	1	
31	188.9	48	1	
32	189.5	25	2	
33	195.3	44	1	

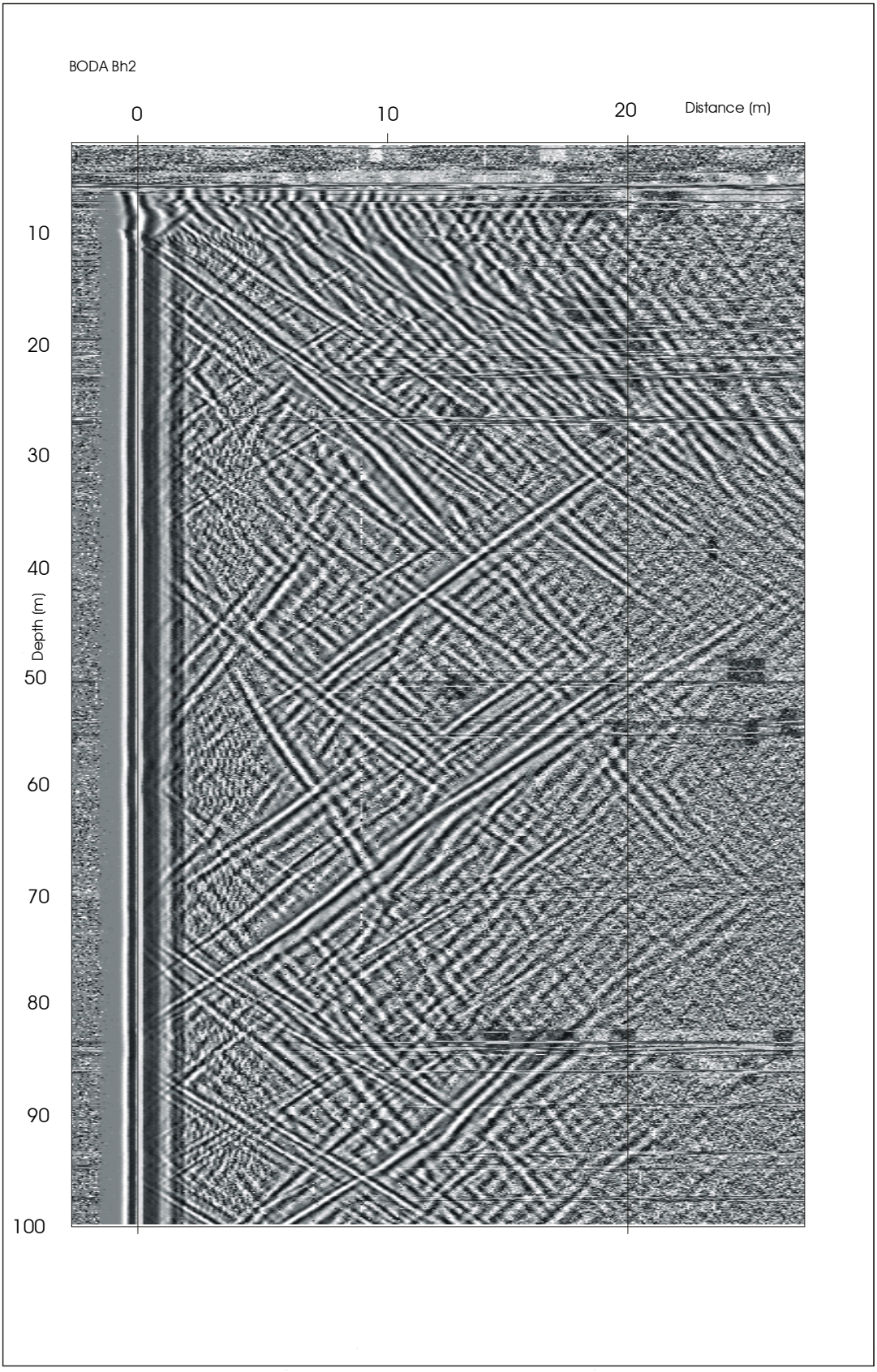

Figure 3-6. Radar reflection map from borehole 2 (0–100 m).

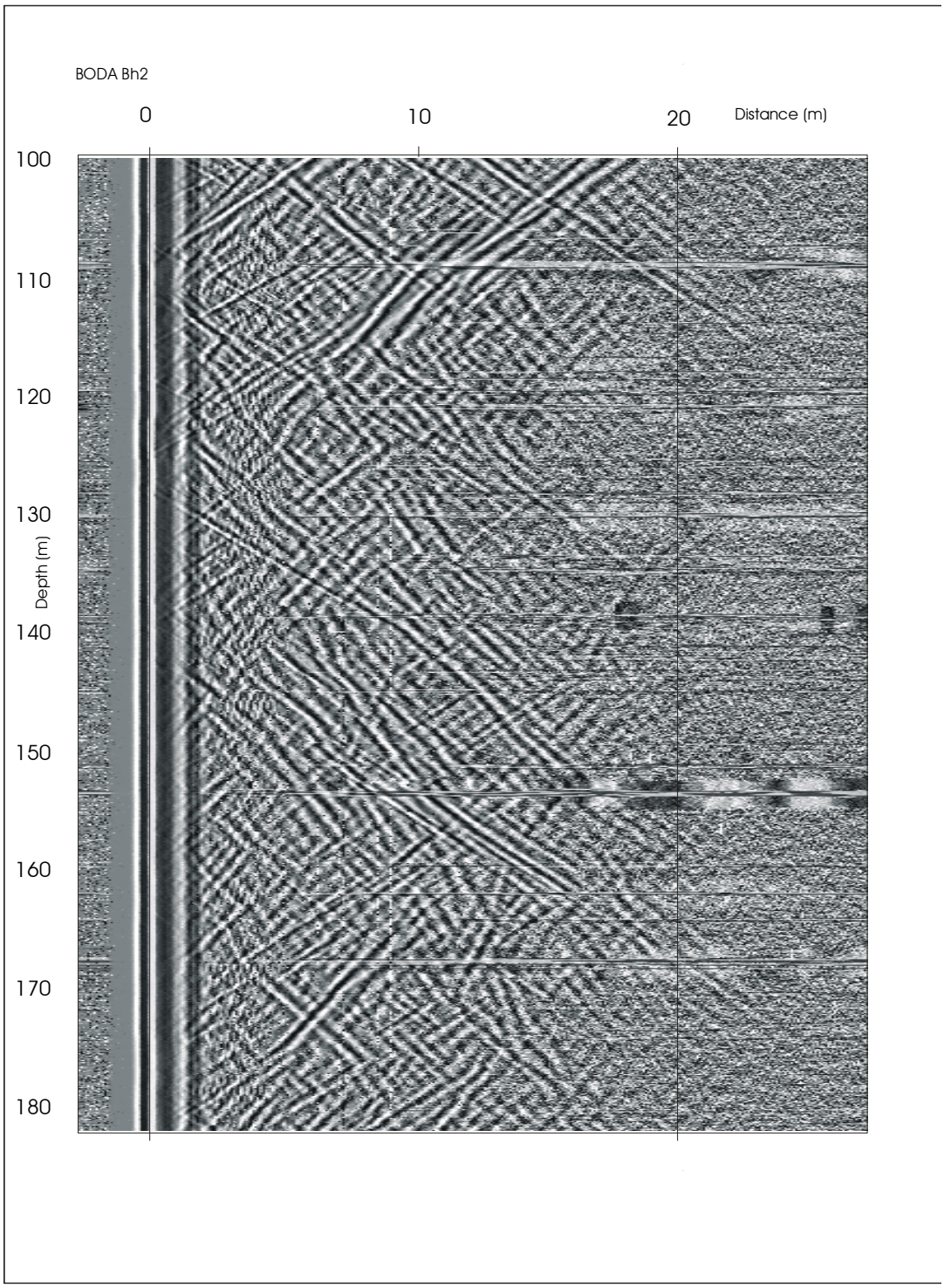

Figure 3-7. Radar reflection map from borehole 2 (100–182 m).

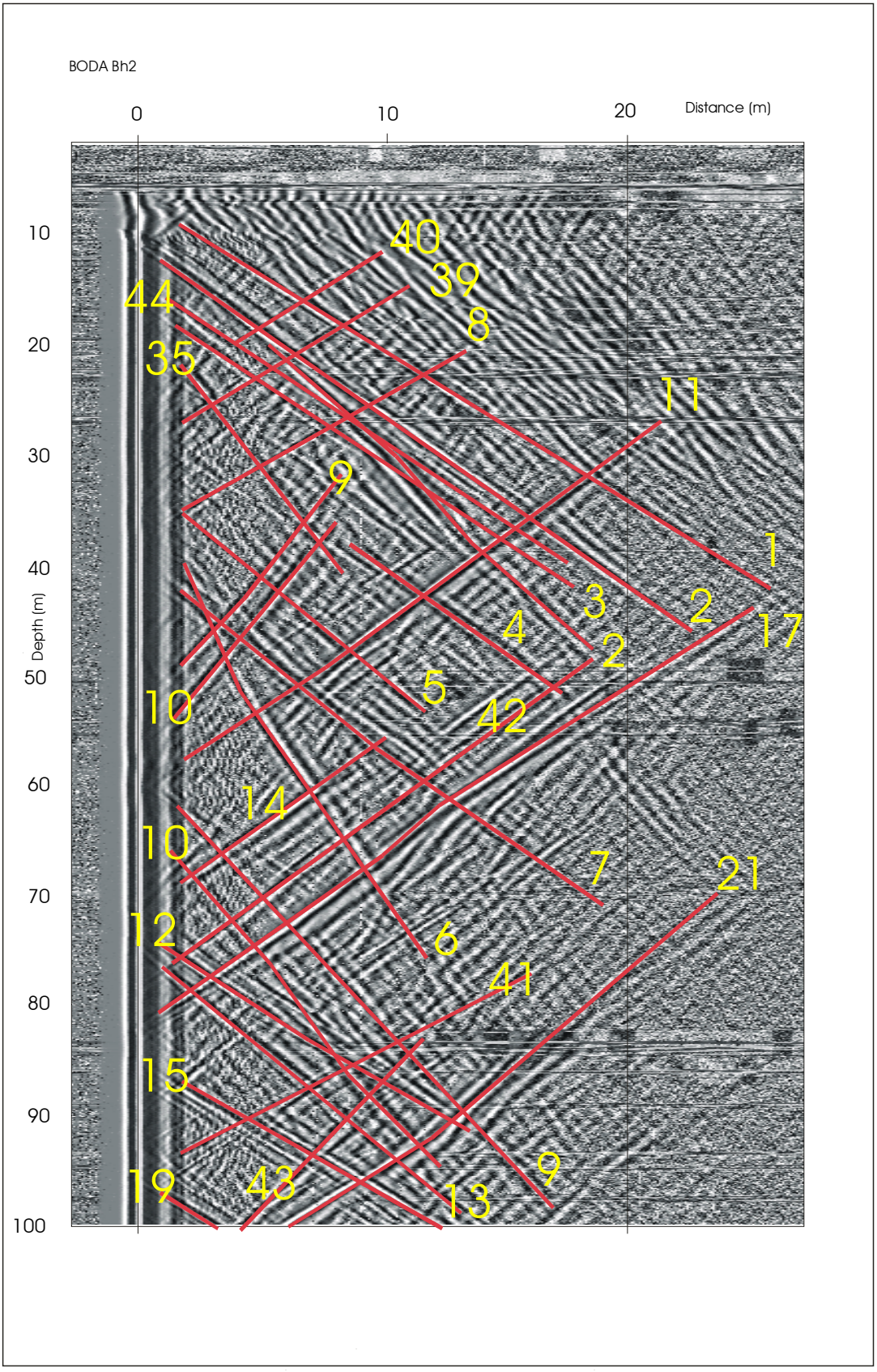

Figure 3-8. Radar interpretation map for borehole 2 (0–100 m).

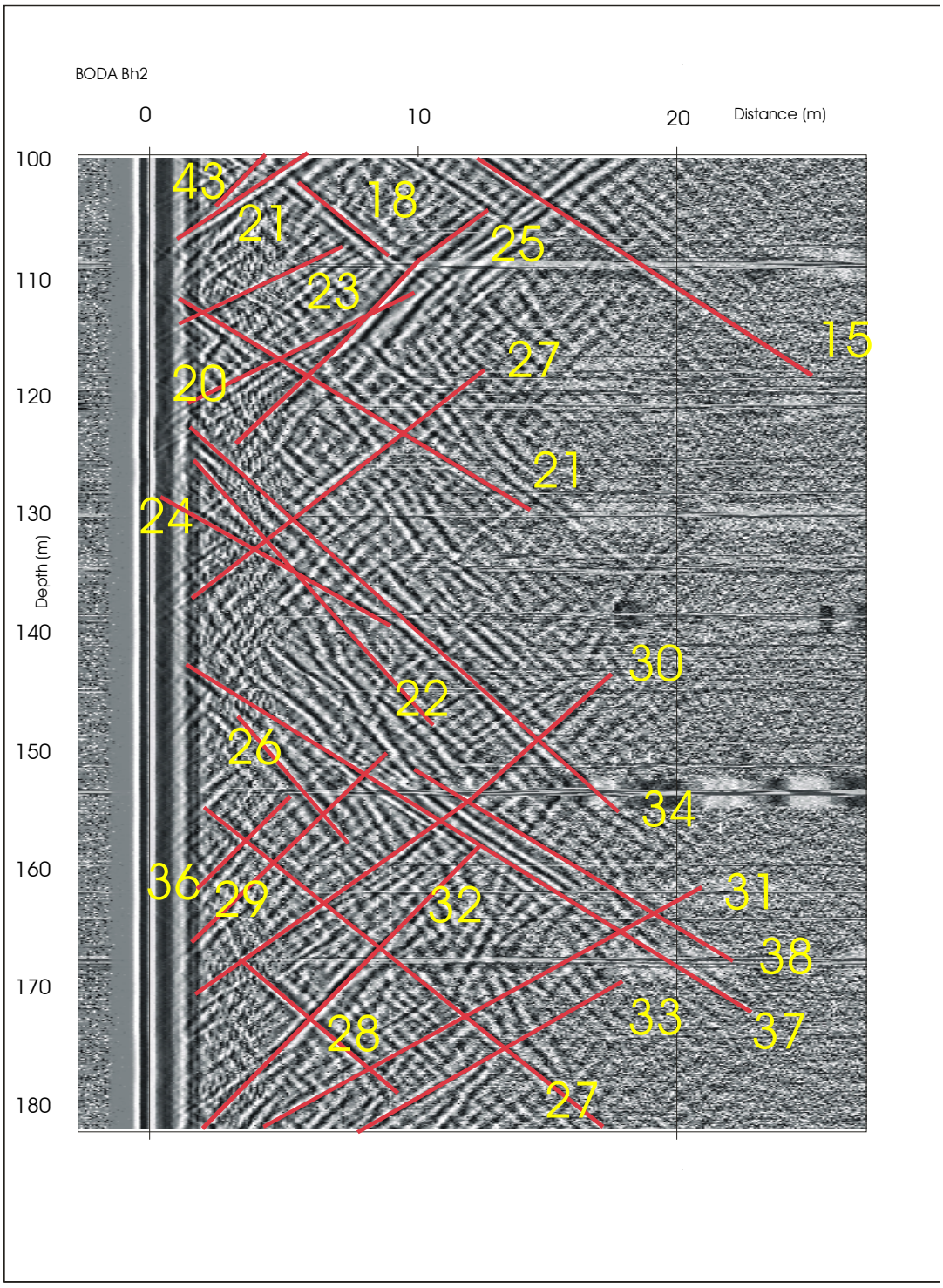

Figure 3-9. Radar interpretation map for borehole 2 (100–182 m).

3.1.7 Results from borehole 3

The dipping borehole 3 was measured from 2.05 meter to 128.6 meter. The quality of the radar measurement is good with a penetration range of radar waves up to 20 meter around the borehole. In some parts of the borehole the penetration range is as much as 25 meter. A radar map from the borehole is presented in Figure 3-10 to 3-11 and the interpretation of the radar map is shown in Figure 3-12 to 3-13 and in Table 3-4.

Several reflectors (structures) are having a strong character in the radar map, and some of them can be traced over large distances. There are many prominent reflectors in the radar map, and some examples can be reflectors 1, 6, 22, and 21. There is a point reflector at borehole length 22.1 meter and at a distance of 2.7 meter from the borehole. This point reflector might indicate the presence of a cave at a vertical depth of about 9 meter (related to top of casing).

An interesting feature is shown by reflector 6, which seems to be divided when followed from 3 meter outside the borehole and upwards. However, there is a possibility that the division of the reflector actually represents two different structures.

Table 3-4. Results from radar investigation in borehole 3.

Reflector ID	Length of intersection related to TOC (m)	Angle of intersection (deg.)	Magnitude 1=weak 2=medium 3=strong U=uncert.	Comments
1	4.6	56	3	Undulating
2	10.1	36	2	Short
30	16.1	39	2	
3	19.4	37	2	
4	21.4	35	1	
P3	22.1		3	Point reflector at a distance of 2.7 m from the borehole
26	22.4	15	1	
28	25.6	15	1	
5	26.8	21	1	
32	29.0	51	1	
6	44.5	31	3	
21	46.5	35	3	
8	49.8	38	2	Short
22	52.9	48	2	
7	56.9	34	2	
9	63.7	33	2	
10	67.0	33	2	
12	71.1	35	2	
11	72.4	13	2	Undulating
13	73.8	39	2	
33	76.0	36	3	
27	76.7	35	1	
14	87.4	36	2	Undulating
23	96.8	35	2	
16	101.8	18	2	Undulating
24	102.9	24	2	Short
15	104.8	15	2	
17	107.6	27	2	Undulating
31	107.8	55	1	
18	114.0	29	2	
25	121.5	33	1	
29	137.1	20	1	
20	151.0	33	2	
19	157.8	32	2	

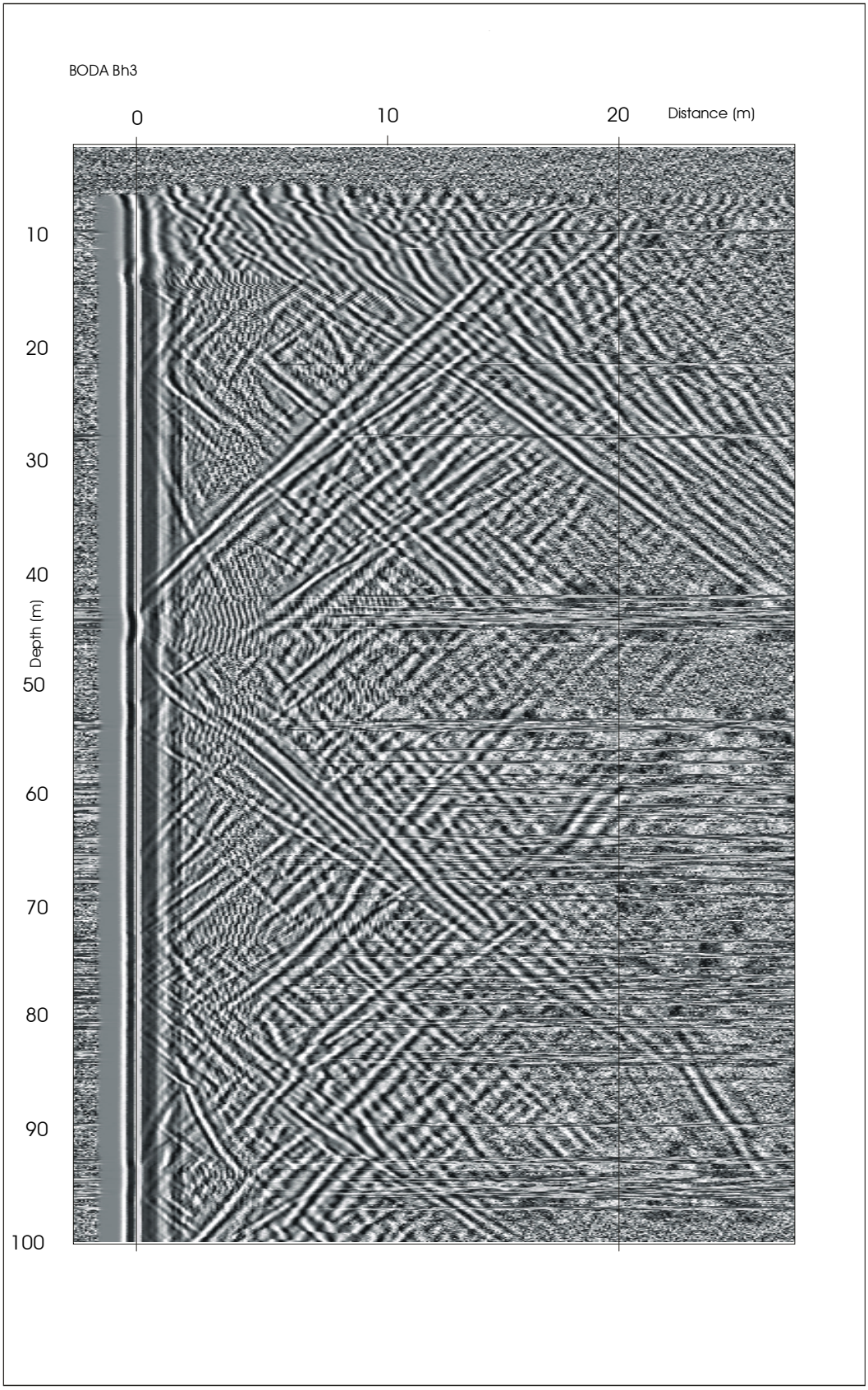

Figure 3-10. Radar reflection map from borehole 3 (0–100 m).

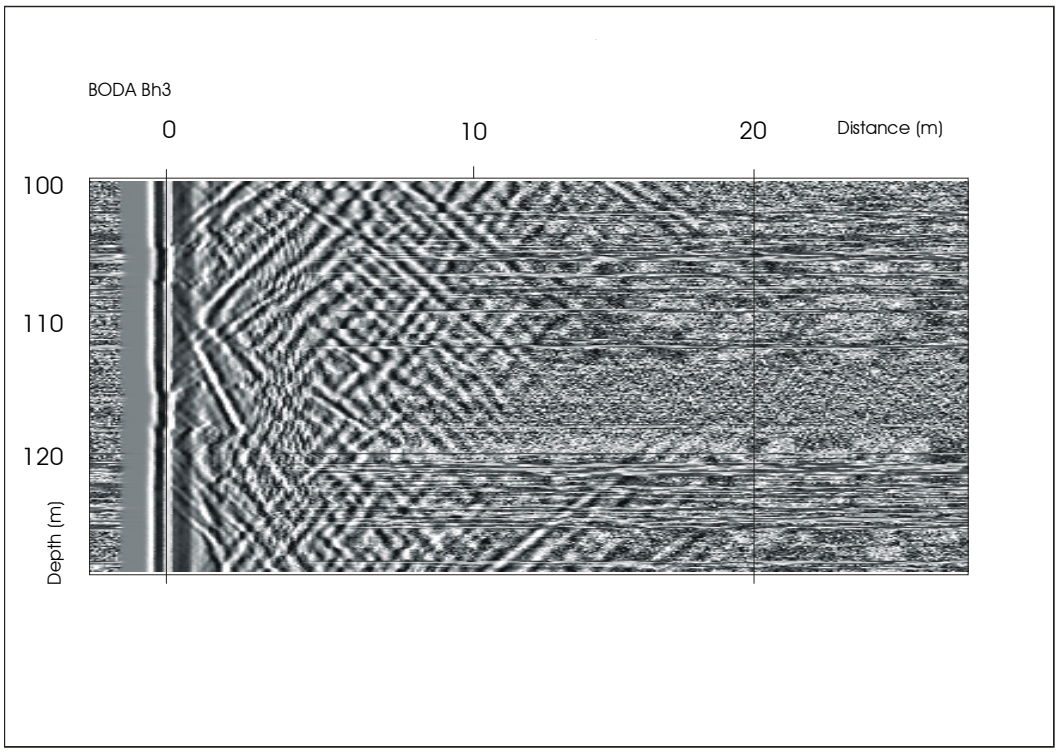

Figure 3-11. Radar reflection map from borehole 3 (100–130 m).

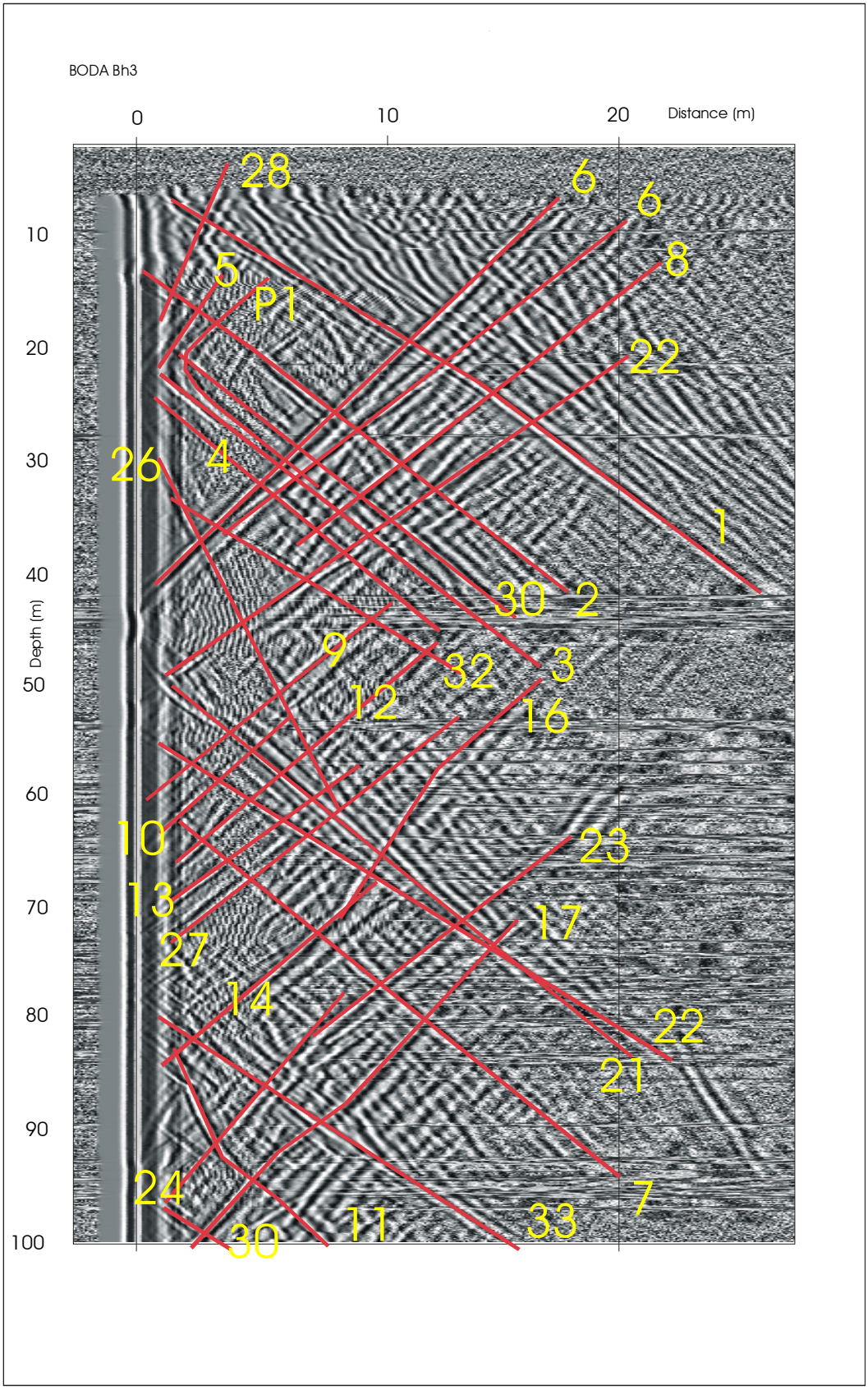

Figure 3-12. Radar interpretation map for borehole 3 (0–100 m).

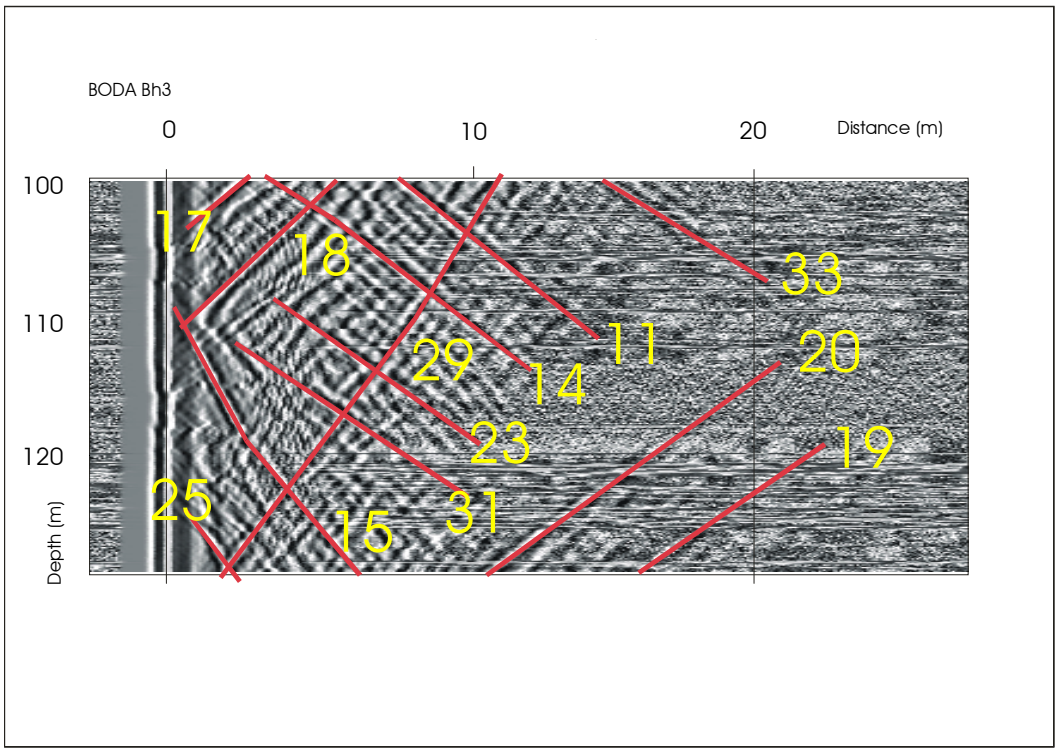

Figure 3-13. Radar interpretation map for borehole 3 (100–130 m).

3.1.8 Results from borehole 4

Borehole 4 was measured from 2.05 meter to 94.7 meter. The quality of the radar measurement is good and the penetration of radar waves around the borehole reach up to 20 meter. A radar map from the borehole is presented in Figure 3-14 and the interpretation of the radar map is shown in Figure 3-15 and in Table 3-5.

From the radar map it can be seen that there are several reflectors (structures) that are exhibiting a strong character in the radar map. Some of them can be traced over large distances. Reflectors 1, 2, 20, 4, 12, and 17 can be mentioned as strong and prominent radar reflectors.

Table 3-5. Results from radar investigation in borehole 4.

Reflector ID	Length of intersection related to TOC (m)	Angle of intersection (deg.)	Magnitude 1=weak 2=medium 3=strong U=uncert.	Comments
1	–6.5	18	3	
20	5.4	21	2	
2	6.3	69	2	
18	18.5	57	1	
24	21.7	90	1	
22	22.2	49	1	
3	22.6	55	1	
4	24.1	21	3	Upper and lower limit of the same structure
	26.8	20	3	
23	28.5	44	1	
26	37.0	64	1	
25	41.3	15	2	
7	48.7	20	2	
5	49.6	26	2	
11	55.5	56	2	
8	56.0	18	2	
6	57.1	16	2	
9	57.6	20	2	
10	58.8	14	2	
19	75.0	26	1	
21	80.8	17	1	
12	84.9	60	1	
14	90.3	21	2	
13	92.3	11	2	
15	103.2	49	2	
16	104.2	53	1	
17	128.0	27	3	

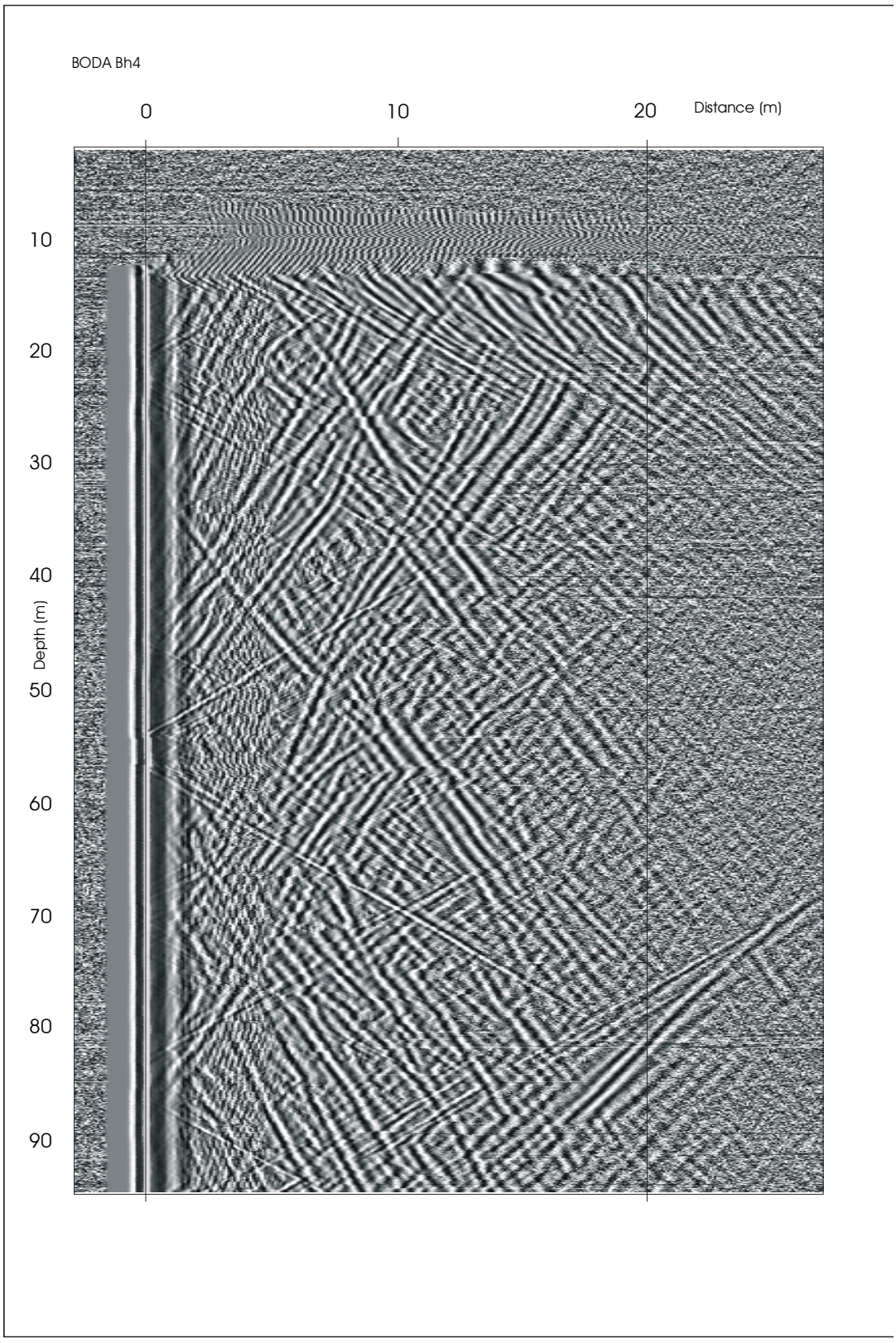

Figure 3-14. Radar reflection map from borehole 4.

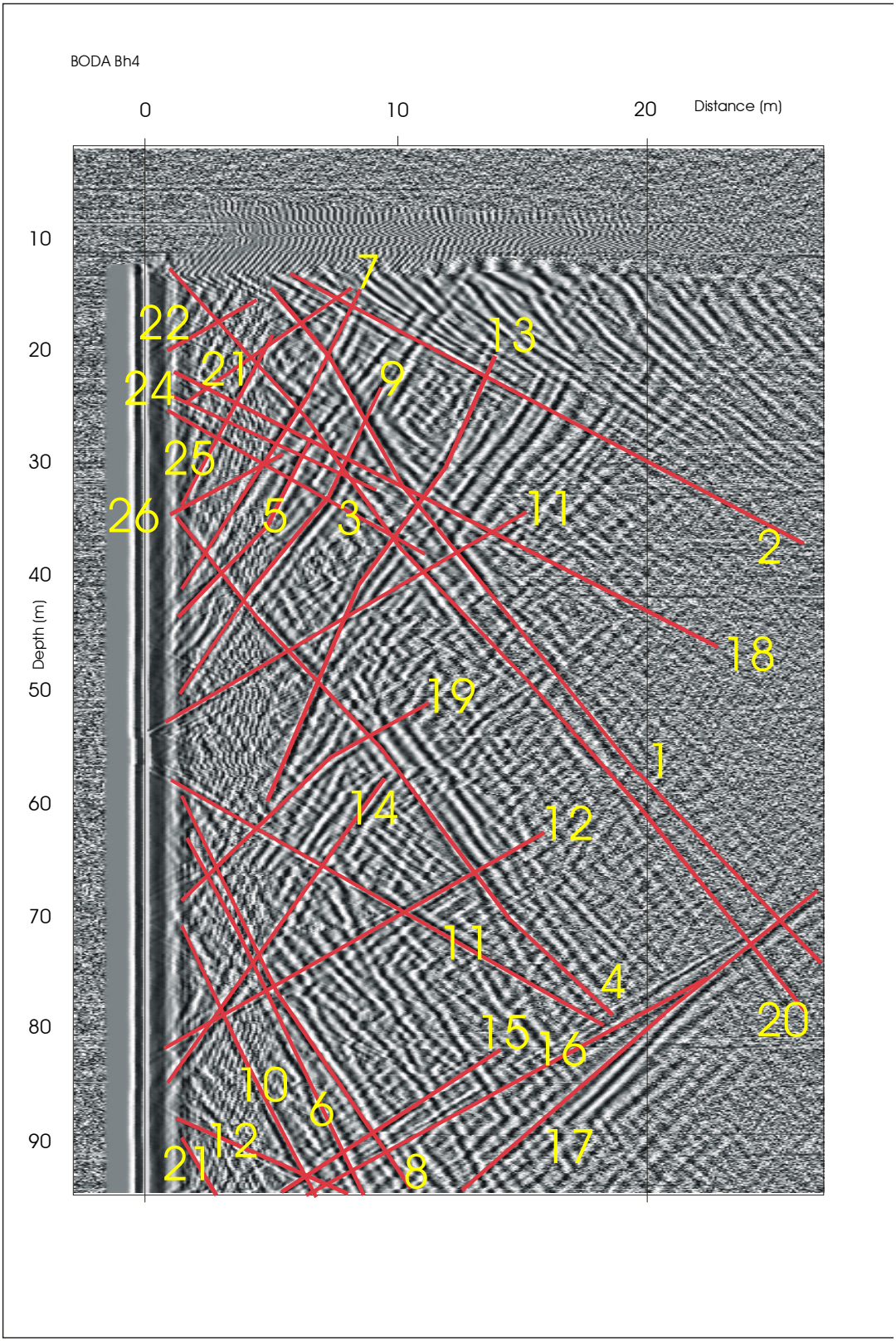

Figure 3-15. Radar interpretation map for borehole 4.

3.2 BIPS measurements

In order to explore the rock beneath the caves at Boda, percussion drilling in combination with BIPS measurements was used to investigate if any structures that could be related to the structures forming the caves could be found. Surface mapping of the rock in the cave area shows the presence of moderately foliated gneiss, with long and narrow near vertical pegmatite dykes. The same pattern was also discovered by the BIPS investigation beneath the cave area.

3.2.1 Short description of the BIPS method

The BIPS method for borehole logging is characterised by the flat continuos 360° colour image, which is produced during logging. The image of the cylindrical borehole wall can be described as a rolled out carpet, where the high side of an inclined borehole is in the centre of the image and the low side is split in the middle and displayed in the left and right end of the image. In a vertical borehole the centre represents the most northern part of the borehole wall. Consequently the lowermost or southernmost parts are represented by the outer edges to the left and right of the out rolled image.

A cylindrical probe with a downhole looking TV camera facing a conical mirror, which reflects the borehole wall into the camera, is with a constant speed lowered down along the borehole. Images from the TV camera are grabbed by a trigged pulse code wheel, which also guides the probe cable. An image processor converts the "cylindrical" image to an ordinary planar image. This image is then stored on MO-disks (magnetic-optical).

As the high or north side of the image is known, the orientation of all structure planes within the borehole can be calculated, provided that the borehole direction is known.

3.2.2 Operation procedure

The borehole is logged downwards with a speed of maximum 1.5 m/min. As the probe is lowered down the borehole, a raw circular image, like looking down a funnel, is shown on a monitor in the field unite. Another monitor shows the planar processed image simultaneously. As the images with normal resolution occupy about 1 MB/m and the MO-disks can store 230 MB, it is possible to log about 200 m in one session. During the logging it is possible to observe fractures and veins on the monitors, as the probe passes them.

After the logging, the files stored on MO-disks are transferred to a PC equipped with mapping software for orientation and mapping of structures in the borehole. Any planar structure crossing the borehole can be oriented and characterised in the mapping process. These planar structures have a sinus-curved appearance on the out rolled borehole wall image. By putting small markers on the sinus shaped structure, the system can calculate a structure orientation in reference to the borehole direction. The borehole orientation, i.e. drilling direction or deviation measurements are used as reference for the orientation calculation of the mapped structures. The apparent width is measured by calculation of the distance between two small markers placed on the edges of the structure.

Table 3-6. Standard characterisation chart.

	Sort	Form	Condition	Remark
0	Primary structure	Planar	Weathered	Quartz
1	Fracture	Undulating	Dull	Chlorite
2	Vein	Stepped	Cavities	Calcite
3	Fracture zone	Irregular	Open	Epidote
4	Contact	Network	Oxidized	Hematite
5	Structure	Breccia	Chloritisized	Pyrite
6	Alteration	Shear	Epidotized	Hybrid rock
7		Crushed	Tectonized	Clay
8		Flow structure		Granite
9		Foliation		Pegmatite
10				Aplite
11				Mylonite

The characterisation of structures is performed by using a standard characterisation chart (Table 3-6). Sort, form, condition and remark are the four groups for characterisation. Sort describes the sort of structure, like fracture, vein or contact. Form describes the form of the structure, like planar, undulating or irregular. Condition describes the condition of the structure, like weathered, oxidised or open. Remark described the filling in the structure, like chlorite, quartz or aplite.

All mapped structures were plotted in stereo nets, one for each borehole and one for the whole area. Sampling along a borehole produces a bias, as the structures which are parallel to the borehole are poorer represented than structures perpendicular to the borehole. The structures have therefor been given a weight in proportion to the angle with which it is cut by the borehole. This value (the Terzaghi value), range from one to infinity, but is here limited to a maximum of five, in order not over compensate the parallel structures.

3.2.3 Results from borehole 1

The fractures beneath the cave area can be separated into two distinct orientations. One dominating subhorizontal fracture set with a small tendency to easterly strike, dipping somewhat towards S. The other minor fracture set strikes N and dips steeply towards E. Almost all open and partly open (cavities) fractures are subhorizontal.

The pegmatite dykes are striking E, dipping intermediately towards south, and showing an apparent width of 10–20 cm.

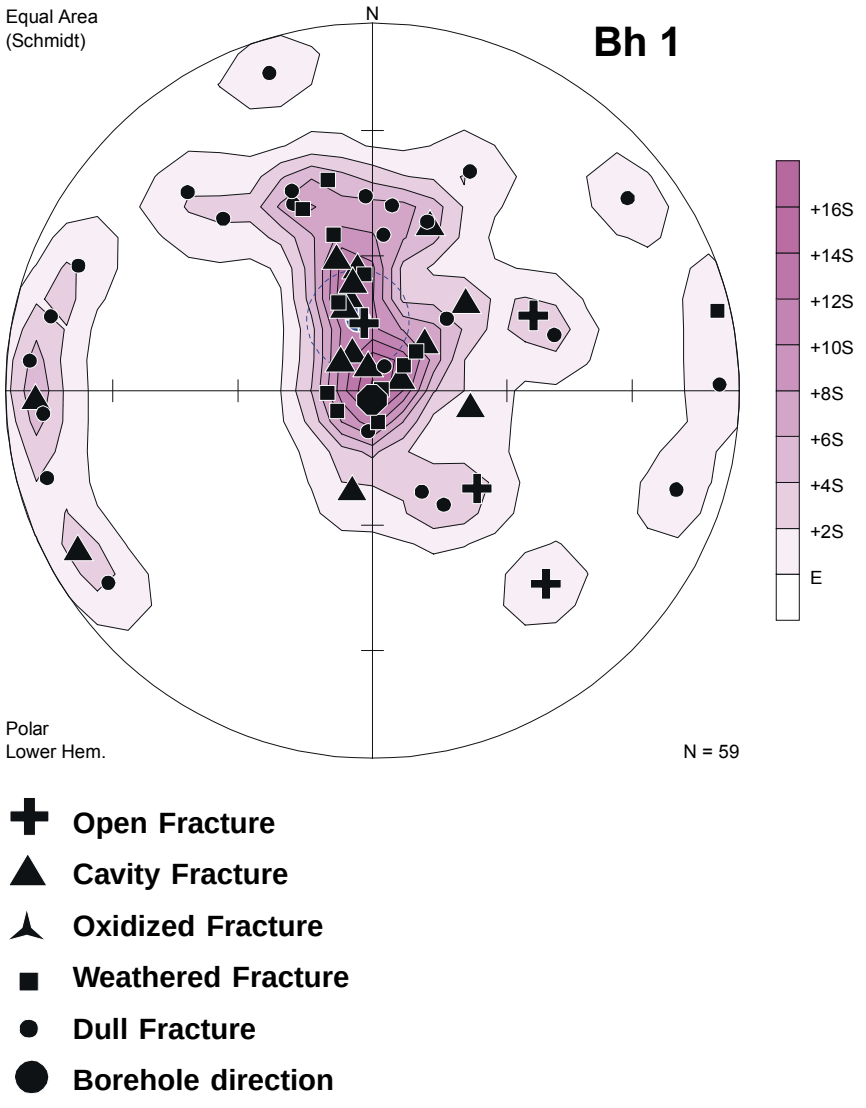

Figure 3-16. All fractures in borehole 1 at the Boda site.

3.2.4 Results from borehole 2

The fractures in borehole 2 can be separated into three distinct orientations. One diffuse subhorizontal fracture set with all of the open fractures. One steeply dipping, NW striking fracture set is dominated by cavity fractures. The cavity fractures occur in both these sets. The pegmatite dykes are gathered in a set striking E and dipping steeply towards S, showing an apparent width of 5–20 cm.

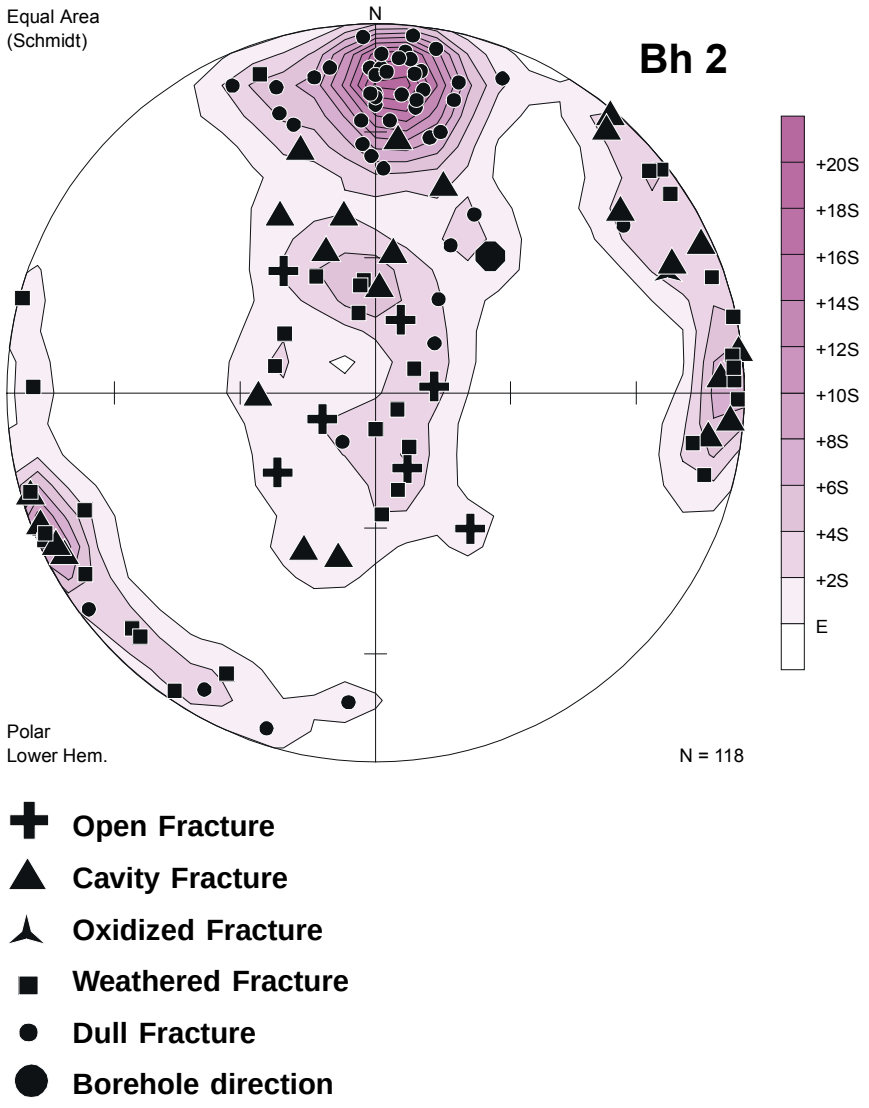

Figure 3-17. All fractures in borehole 2 at the Boda site.

3.2.5 Results from borehole 3

The fractures in borehole 3 can be separated into three distinctly oriented fracture sets. One subhorizontal, another striking S and dipping steeply towards W and the third, with most of the dikes, striking ESE dipping towards S. In this borehole, two sets of open and partly open (cavities) fractures are present, one subhorizontal and one striking S, dipping steeply towards W.

The pegmatite dykes are here striking ESE and dipping steeply towards S, showing an apparent width of 5–25 cm.

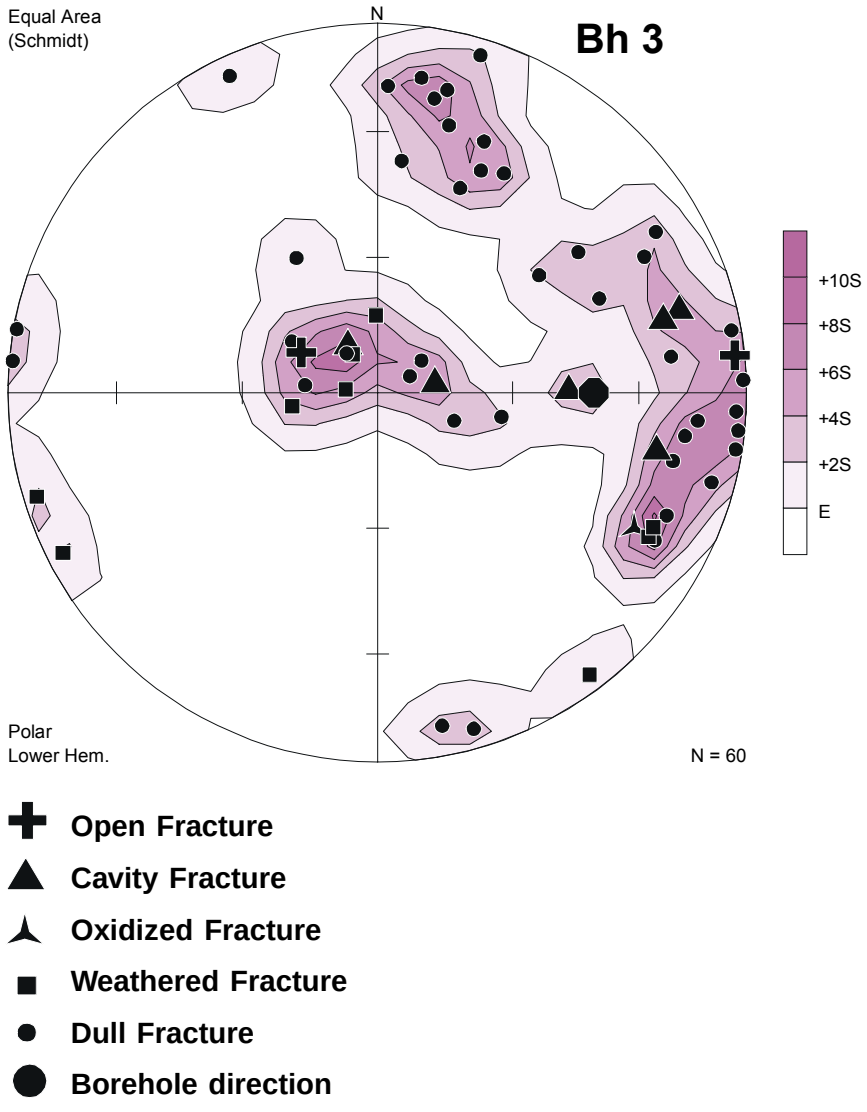

Figure 3-18. All fractures in borehole 3 at the Boda site.

3.2.6 Results from borehole 4

The fractures in borehole 4, show one dominating subhorizontal set. Accordingly the open and partly open (cavities) fractures are also subhorizontal.

The pegmatite dykes form a group, which is striking ESE, dipping steeply towards S, and showing an apparent width of 5–25 cm.

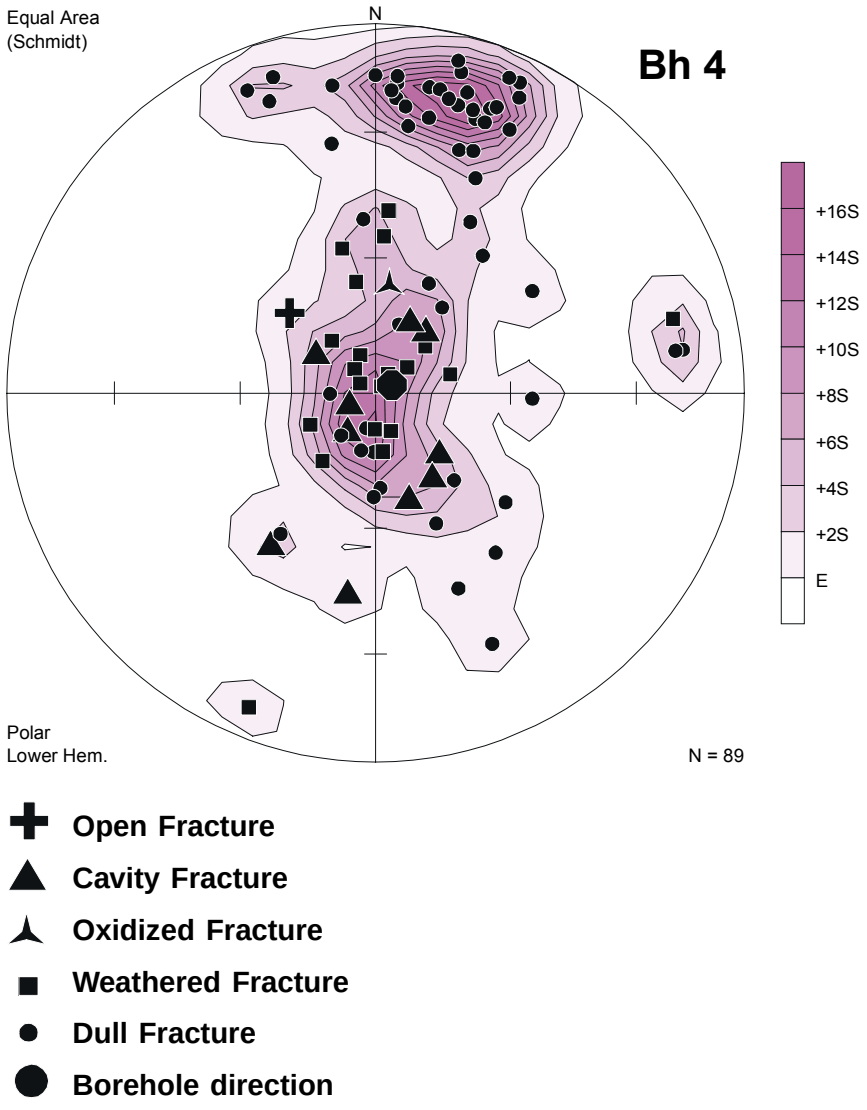

Figure 3-19. All fractures in borehole 4 at the Boda site.

3.2.7 Number and orientation of fractures and veins in the boreholes

From the data collected during the BIPS mapping, fracture and vein data can be extracted for statistical analysis. Tables 3-7 and 3-8 show the number of fractures and veins in the boreholes. Table 3-9 shows the orientation of fractures and veins in each borehole. For fractures it also shows if there are fracture sets with different orientations.

Stereo diagrams (Schmidt-net) showing the dominating fracture and vein orientation in the rock volume, penetrated by the boreholes, where produced. The diagrams show the orientation for all structures: Borehole 1 (Figure 3-16), Borehole 2 (Figure 3-17), Borehole 3 (Figure 3-18) and Borehole 4 (Figure 3-19). In Figure 3-20 the orientation of all structures in all four boreholes are gathered.

In the stereo diagrams the normal of the fracture or vein planes are plotted on the lower half of a sphere, and observed from above.

Table 3-7. Number of fractures and veins.

	Borehole 1	Borehole 2	Borehole 3	Borehole 4	All Boreholes
All Fractures	42	68	33	41	184
Open & Cavities	20	31	8	11	70
Veins & Dykes	10	44	21	34	109

Open = open fractures

Cavities = partly open fractures

Table 3-8. Number of open and cavities in 10 metres section in the boreholes.

Borehole section	Borehole 1	Borehole 2	Borehole 3	Borehole 4
0–10	1	2	0	0
10–20	3	2	2	2
20–30	0	0	0	5
30–40	4	0	0	0
40–50	3	0	1	1
50–60	1	1	1	1
60–70	2	1	1	0
70–80	2	3	1	1
80–90	4	1	1	0
90–100		1	0	
100–110		7	1	
110–120		2		
120–130		4		
130–140		3		
140–150		2		
150–160		2		

Table 3-9. Orientation of fractures and veins.

	Borehole 1	Borehole 2	Borehole 3	Borehole 4	All Boreholes
All Fractures	SH/S, N/E	SH, NW/90	SH, S/W	SH	SH, N/90
Open & Cavities	SH	SH	SH, S/W	SH	SH, NNW/90
Veins & Dykes	E/S	E/S	ESE/S	SE/SW	ESE/S
Borehole direction	184/88	40/50	90/41	64/86	–

SH = subhorizontal

Open = open fractures

Cavities = partly open fractures

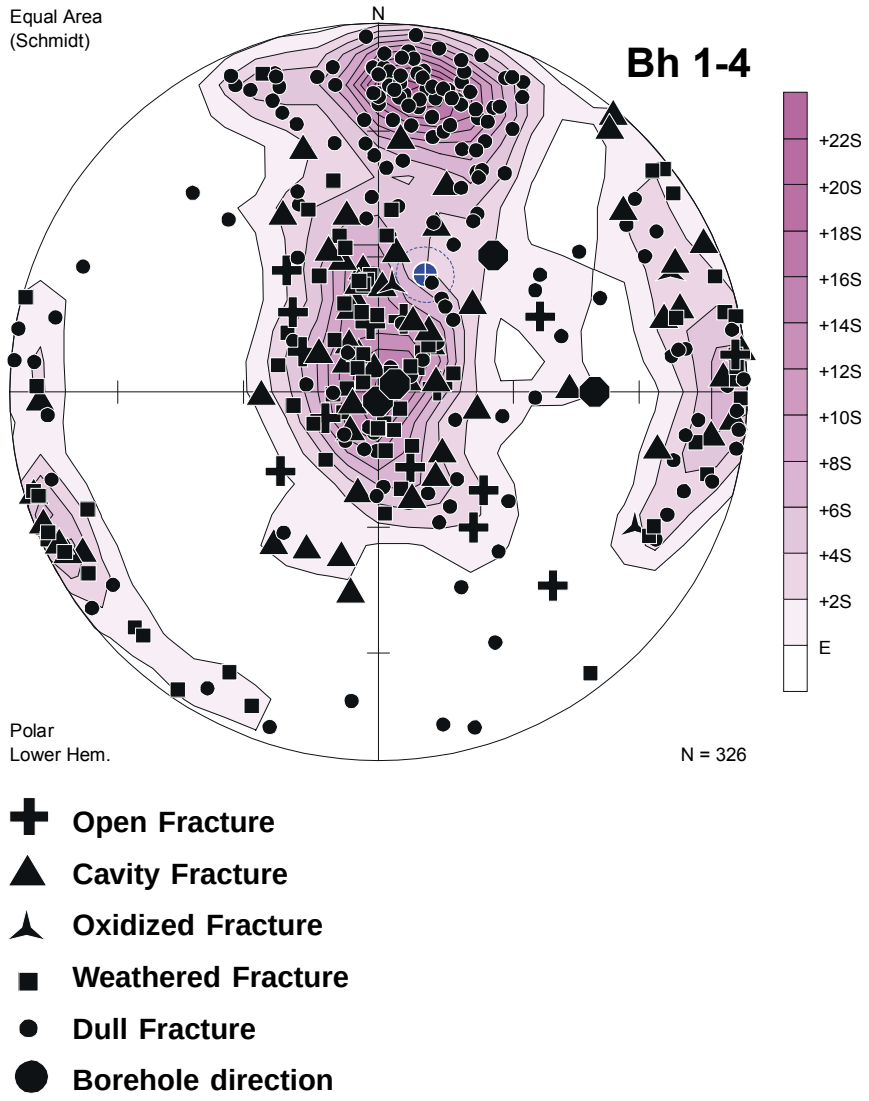

Figure 3-20. All fractures in all four boreholes.

By combining all structures from all four boreholes in one stereo diagram (Figure 3-20), it is possible to see the character of the whole rock volume penetrated by the boreholes. The impression from the separate boreholes remains. The site is dominated by three sets, where one is dominated by pegmatite veins (E-ESE/60–90°). A subhorizontal set where we find almost all open fracture and many of the cavity fractures. And finally a steep set striking north to northwest (N-NW/90°) with a lot of the cavity fractures.

The most prominent open fractures discovered in the boreholes are subhorizontal to gently dipping. The steeper fractures are not so wide and spectacular as the more horizontal ones. The widest open fracture observed has an apparent aperture width of 133 mm and a strike and dip of 43/26 (see Figure 3-21).

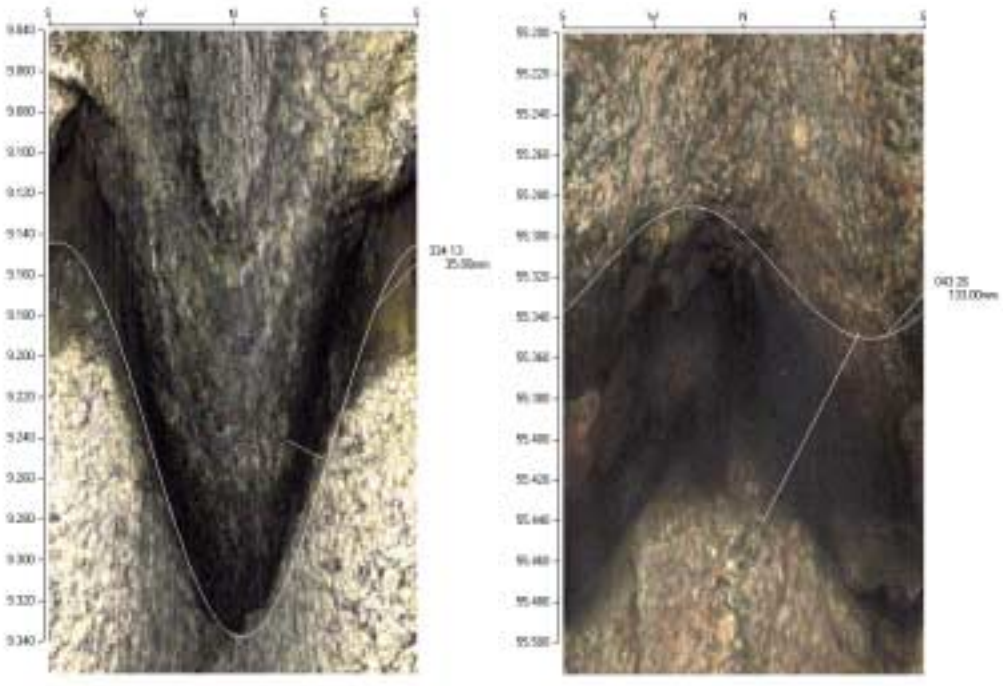

Figure 3-21. Examples of open fractures with large apparent apertures (133 mm was the largest) that was discovered beneath the cave area.

The 14 open fracture apertures varies between 6 and 133 mm. Figure 3-22 shows that the majority of the open fractures are dipping subhorizontally to gently (10–40°). Only two fractures have steeper dip.

The vertical distribution is rather uniform, with some tendency to small accumulations around 5 m, –40 m and –70 m from sea level (see Figure 3-23). The fracture with the apparent aperture of 133 mm, is located at about –40 m.

The truly visible pegmatite dykes seen on the surface are also present at depth of this investigation. The pegmatite dykes have a very steady orientation striking E and dipping about 75° to the S (Figure 3-24).

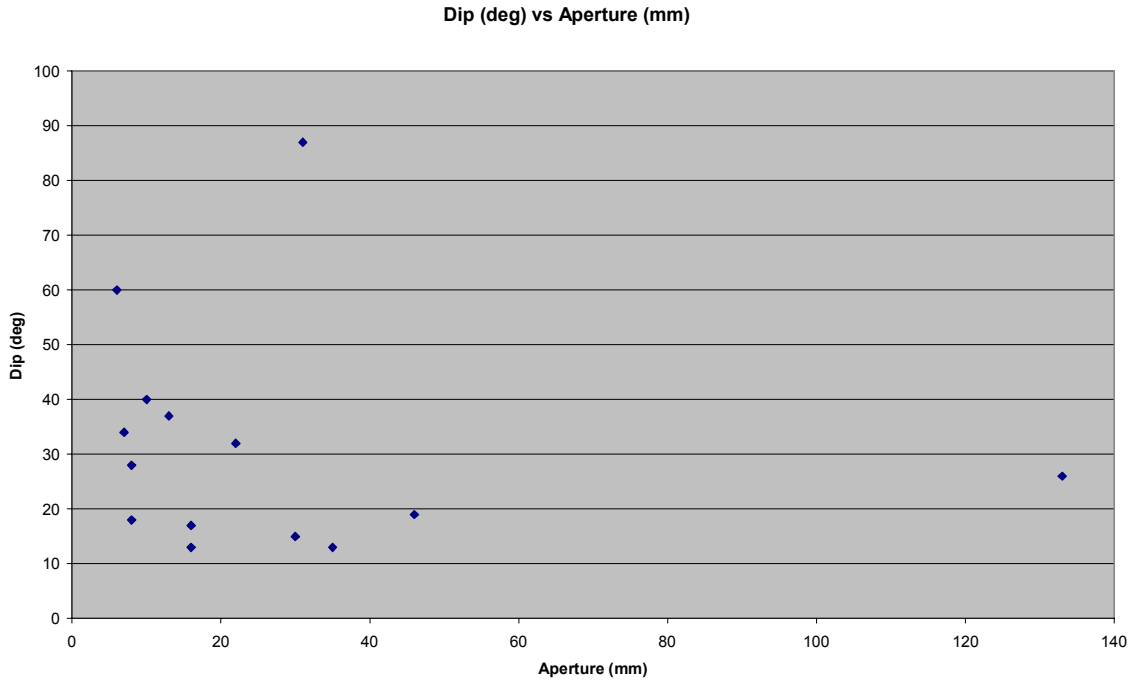

Figure 3-22. The apparent aperture of open fractures plotted against the dip.

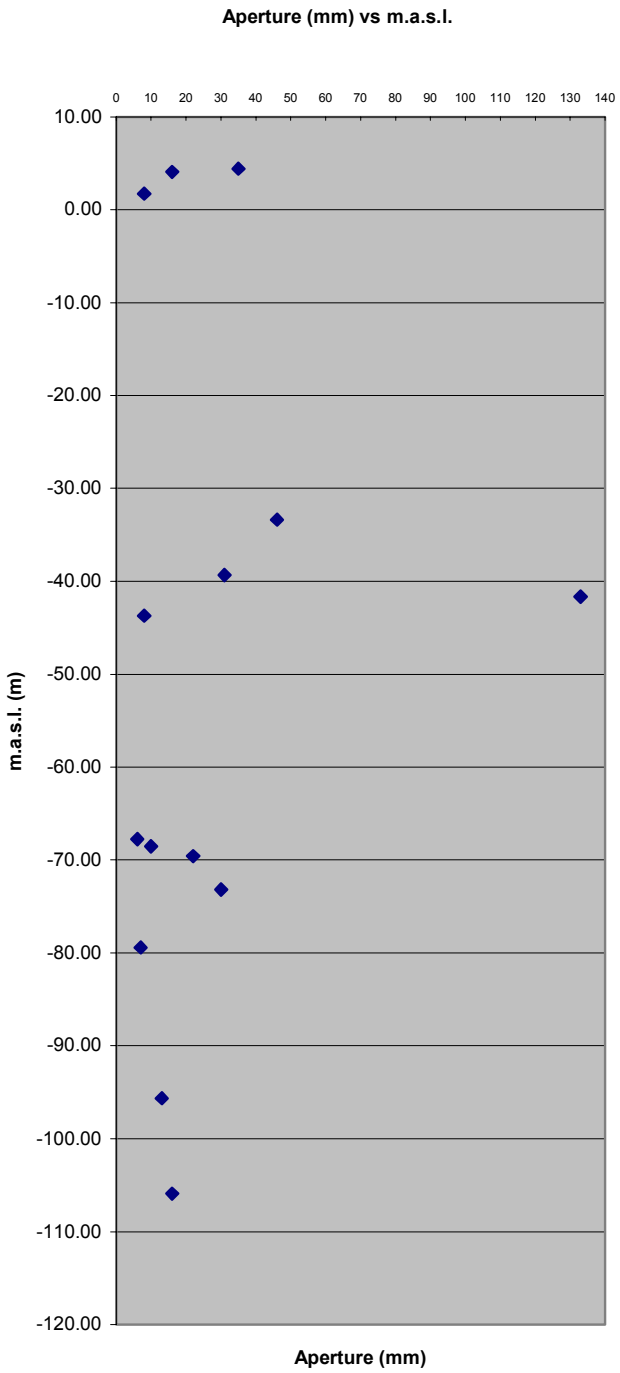

Figure 3-23. The apparent aperture of open fractures plotted against vertical depth (m.a.s.l.).

Figure 3-24. The pegmatitic veins are clearly oriented E/70–80°.

3.2.8 Block size

The average distance between cavities and open fractures within the subhorizontal set, is about 5.6 m in borehole 1 and 6.8 m in borehole 4.

The average distance between cavities and open fractures within the vertical set, is about 11.6 m in borehole 2 and 11.3 m in borehole 3.

These values suggest a prismatic bloc, with the size in the order of 11 m wide and 6 m high.

Pegmatite veins appear very distinctly with an easterly strike, dipping 70–80° towards south. The average distance between the pegmatite dykes is 3.3 m in borehole 2 and 7.4 m in borehole 3. The value 7.5 m, is probably the most accurate due to borehole 3 having the most optimal borehole direction.

4 Comparison between radar reflectors and BIPS-structures

BIPS gives information about structures encountered and mapped in the borehole. However, there will be uncertainty about the extent of the mapped structures since BIPS gives no information about that. Borehole radar, on the other hand, gives information about the extent of structures from close to the borehole to several meters outside the borehole. However, borehole radar structures have to be compared to borehole mapping, BIPS-mapping in this case, in order to connect them to geological structures. It is of importance to know whether structures have any extension or if they are of a very local nature. This together gives a possibility to a better understanding of the 3-dimensional pattern.

Two sets of radar data were recorded using different frequencies, 100 MHz and 250 MHz. Best result was achieved with 100 MHz antennas. The data from the 250 MHz was disturbed by a strong ringing of the radar pulse, caused by the large borehole diameter. Consequently, the radar data from 100 MHz measurements have been used as basis for interpretation and presentation in the report.

Dipole antenna radar reflectors have been the basis for the comparison between reflectors interpreted by dipole radar antenna and structures logged and oriented using BIPS. The result of the comparison is presented in a table for each borehole. It should be noted that the accuracy of intersection length with borehole is less for radar reflectors compared to BIPS-mapped structures. Also, the accuracy of intersection length is less for radar reflectors having a small angle to borehole axis, compared to radar reflectors having a large angle to borehole axis.

The quality of the radar measurements is considered good. The radar maps from the four percussion drilled boreholes contain a large number of strong and prominent reflectors. The prominent reflectors can be traced over large distances in the radar maps. This indicates that the structures in the area are rather continuos. The borehole radar provides information around the borehole in a radius ranging from 1–2 meter to 20–25 meter. Only one point reflector was observed in the radar maps. Point reflectors might indicate open cavities in the surrounding rock mass. The point reflector was found in borehole 3 at a rather shallow vertical depth, namely about 9 m below ground level. The absence of point reflectors at larger depths around the boreholes does not support the presence of caves at larger depths in the area.

The quality of the BIPS measurements is also considered good. However, in the lowest part in borehole 2, 3, and 4, particles in suspension deteriorated the visibility and only larger structures were possible to be mapped. BIPS has revealed a dominating subhorizontal fracture set. Another set strikes NW to N-S with a dip close to vertical. Possible but very uncertain is a fracture set striking NE and dipping steeply towards S. The open and partly open fractures forms an average blocksize with the dimensions 11 m wide and 6 m high. The length of the block is uncertain.

A total number of 98 radar reflectors were included in the comparison procedure, i.e. those intersecting the borehole where BIPS-logging and mapping was performed. BIPS mapping was not possible in the deepest part of some boreholes due to muddy borehole water. Of the 98 radar reflectors 90 were combined with BIPS-structures. The intersection length and the orientation were used as basis for this combination. Importance was put on the a-angle of the radar reflector and the BIPS-structure. The a-angle is the angle between borehole axis and the plane of the structure.

Table 4-1. Combination between radar reflectors and BIPS-structures in borehole 1.

Radar reflector ID	Depth of radar reflector (m)	Angle of intersection of radar reflector (degr.)	Depth of BIPS-structure (m)	Angle of intersection of BIPS-structure (degr.)	Orientation of BIPS-structure (dip/strike)	Comments
19	6.9	90	6.6	68	22/282	Fracture 3 mm cavities
4	10.9	16	13.0	14	76/023	Fracture 8 mm
5	15.6	34	14.0	55	35/094	Vein 23 mm
6	18.1	14	15.4	11	79/013	Fracture 6 mm
7	22.5	25	20.9	48	42/096	Vein 37 mm
8	36.8	22	–			
9	37.7	60	37.7	61	29/136	Fracture 24 mm cavities
17	43.6	28	–			
10	54.7	46	53.6	68	22/076	Fracture 5 mm cavities
20	65.4	41	65.0	41	49/078	Fracture 4 mm cavities
23	76.4	50	76.0	59	76/143	Fracture 1 mm cavities
11	77.3	37	77.1	46	44/069	Fracture 7 mm
13	81.0	17	81.9	6	84/179	Fracture 10 mm
12	82.5	44	81.1	58	32/223	Fracture 22 mm open
18	93.4	32	93.4	46	44/088	Vein 34 mm

Table 4-2. Combination between radar reflectors and BIPS-structures in borehole 2.

Radar reflector ID	Depth of radar reflector (m)	Angle of intersection of radar reflector (degr.)	Depth of BIPS-structure (m)	Angle of intersection of BIPS-structure (degr.)	Orientation of BIPS-structure (dip/strike)	Comments
2	9.2	39	9.2	31	35/259	Fracture 35 mm open
44	13.1	40	12.7	31	18/247	Fracture 8 mm open
3	14.4	40	14.4	26	80/187	Fracture 12 mm cavities
35	15.1	24	–			
4	22.8	40	22.6	42	87/323	Vein 45 mm
40	26.1	51	25.5	41	87/096	Vein 60 mm
5	26.3	31	26.3	37	86/088	Vein 253 mm
6	29.7	15	29.5	16	89/015	Fracture 16 mm
39	31.0	50	31.1	35	85/288	Vein 111 mm
7	37.4	35	37.8	39	82/095	Vein 29 mm
8	39.2	51	39.2	50	76/105	Vein 129 mm
9	55.8	27	56.1	45	80/096	Vein 114 mm
10	60.8	23	59.0	36	13/304	Vein 857 mm
11	63.3	41	66.3	30	88/338	Fracture
12	71.5	42	71.9	26	28/321	Fracture 8 mm open
13	73.4	35	73.2	29	84/333	Fracture 2 mm cavities
14	73.9	39	74.5	32	83/177	Fracture 5 mm cavities
42	80.1	38	79.4	43	76/097	Vein 241 mm
16	82.4	19	83.7	28	81/070	Fracture 11 mm
17	83.7	44	82.8	44	23/015	Fracture 5 mm
15	83.9	50	83.4	78	46/119	Vein 59 mm
18	90.5	35	90.7	45	69/090	Vein 202 mm
19	94.6	52	93.3	71	32/097	Fracture 2 mm
41	96.8	64	97.8	51	75/157	Vein 53 mm
20	108.1	21	107.6	25	81/316	Fracture 10 mm
21	110.1	49	110.0	23	81/065	Vein 251 mm
43	111.3	31	111.0	48	57/087	Vein 16 mm
23	117.2	55	116.8	33	80/094	Vein 30 mm
22	118.6	23	118.3	46	34/053	Fracture 7 mm open
34	119.4	35	118.9	31	87/174	Fracture 10 mm
20	124.7	45	125.1	43	46/062	Fracture 5 mm cavities
24	126.5	54	126.2	31	88/336	Fracture 7 mm
25	131.7	32	131.5	33	76/189	Fracture 5 mm
26	134.7	22	135.1	27	86/184	Fracture 9 mm open
38	138.4	50	138.3	53	62/104	Vein 12 mm
37	139.6	48	139.4	39	37/235	Fracture 13 mm open
27	142.1	33	141.9	42	85/141	Fracture 6 mm

Table 4-3. Combination between radar reflectors and BIPS-structures in borehole 3.

Radar reflector ID	Depth of radar reflector (m)	Angle of intersection of radar reflector (degr.)	Depth of BIPS-structure (m)	Angle of intersection of BIPS-structure (degr.)	Orientation of BIPS-structure (dip/strike)	Comments
2	10.1	36	11.0	34	13/060	Fracture 12 mm cavities
30	16.1	39	15.3	63	70/153	Foliation
3	19.4	37	19.1	66	56/145	Vein 38 mm
4	21.4	35	20.3	23	22/031	Fracture 14 mm
26	22.4	15	23.1	30	64/105	Vein 395 mm
28	25.6	15	23.8	–	–	Lower contact of vein 395 mm
5	26.8	21	24.7	36	63/113	Vein 30 mm
32	29.0	51	28.8	52	83/195	Vein 101 mm
6	44.5	31	44.7	35	70/101	Vein 85 mm
21	46.5	35	46.2	40	53/096	Fracture 3 mm
8	49.8	38	–	–		
22	52.8	48	52.6	23	19/351	Fracture 6 mm irregular
7	56.9	34	56.5	14	85/107	Vein 15 mm irregular
9	63.7	33	62.3	35	07/006	Fracture 5 mm
10	67.0	33	66.7	17	72/092	Vein 296 mm
12	71.1	35	70.9	49	08/153	Fracture 8 mm
11	72.4	13	72.5	25	19/028	Fracture 46 mm open
13	73.8	39	74.8	35	11/052	Fracture 20 mm
33	76.0	36	76.3	49	76/150	Fracture 10 mm
27	76.7	35	76.8	27	16/006	Fracture 10 mm
14	87.4	36	89.1	19	35/059	Vein 22 mm
23	96.8	35	–			
16	101.8	18	–			
24	102.9	24	103.3	15	84/254	Vein 22 mm
15	104.8	15	–			
17	107.6	27	–			
31	107.8	55	108.8	48	88/189	Vein 129 mm

Table 4-4. Combination between radar reflectors and BIPS-structures in borehole 4.

Radar reflector ID	Depth of radar reflector (m)	Angle of intersection of radar reflector (degr.)	Depth of BIPS-structure (m)	Angle of intersection of BIPS-structure (degr.)	Orientation of BIPS-structure (dip/strike)	Comments
18	18.5	57	18.2	58	32/245	Fracture 1 mm
24	21.7	90	21.3	71	19/222	Fracture 2mm cavities
22	22.2	49	21.3	68	22/235	Fracture 1 mm cavities
3	22.6	55	22.1	45	45/278	Fracture 4 mm cavities
4	24.1	21	25.1	8	82/115	Vein 117 mm
23	28.5	44	28.6	49	41/305	Fracture 3 mm cavities
26	37.0	64	37.2	81	09/068	Fracture 1 mm
25	41.3	15	41.6	17	73/094	Vein 183 mm
7	48.7	20	48.4	17	73/172	Contact, upper
5	49.6	26	51.1	32	58/080	Contact, lower
11	55.5	56	55.3	64	26/043	Fracture 133 mm open
8	56.0	18	54.3	15	75/090	Vein 286 mm
6	57.1	16	57.0	23	67/096	Vein 88 mm irregular
9	57.6	20	58.6	18	72/112	Vein 186 mm irregular
10	58.8	14	58.9	22	68/110	Vein 191 mm irregular
19	75.0	26	77.7	11	79/105	Vein 140 mm irregular
21	80.8	17	81.4	8	82/104	Vein 39 mm irregular
12	84.9	60	84.5	57	33/077	Fracture 28 mm
14	90.3	21	89.8	20	70/109	Vein 89 mm

5 Conclusions

In total 124 radar reflectors have been interpreted from the radar maps. Of them 98 are interpreted to intersect within BIPS-logged and mapped sections in the boreholes. It has been possible to combine 90 of the 98 reflectors with geological structures mapped by BIPS. Consequently, there was no explanation for 8 radar reflectors. This means that 92% of all interpreted reflectors intersecting BIPS-mapped sections have been combined with BIPS-structures. Possible explanations for the remaining 8% of radar reflectors not combined with BIPS-structures may be (i) BIPS do not detect all structures, (ii) some radar reflectors can be conditioned by mineralogical contents such as biotite, sulphides, etc, (iii) some radar reflectors indicate structures detected outside the borehole, (iv) some radar reflectors might bend and intersect the borehole at a borehole length other than the radar interpreted.

The BIPS measurement shows the presence of 14 open fractures, but there is no evidence of fractures large enough to form caves at the depth in the area.

The borehole radar shows that the open fractures and other structures have an extension of tens of meters away from the boreholes. Cavities in the rock mass are normally seen as point reflectors in a radar map. The borehole radar maps from Boda show no evidence of caves at depth in the area.

The fractured rock around Boda is a shallow feature, since borehole radar and BIPS measurements shows no evidence of increased fracturing or the presence of caves at larger depth in the Boda area. The conclusion from this investigation indicates that the formation of the superficial fracture system (with caves included) at Boda in all probability is connected to glacial action, such as banking.

References

Wänstedt S, 2000. Geophysical and geological investigations of the Boda area. SKB R-00-23, Stockholm, Sweden.

Sandberg E, Olsson O, Falk L, 1991. Combined interpretation of fracture zones in crystalline rock using single-hole, crosshole tomography and directional borehole-radar data. The Log Analyst, 32(2), 108–119.

Appendix 1

Deviation measurements in boreholes at Boda

x = Total displacement in principal coordinate axis direction.
y = Total displacement in direction 90 degrees clockwise from X.
z = True vertical depth.
Principal coordinate axis is given in degrees (0–360) measured clockwise from magnetic north. All distances in meter. Azimuth 0–360 degrees from principal coordinate axis.

Borehole 1

Station (m)	Dip (degrees)	Azimuth (degrees)	x (m)	y (m)	z (m)
10	−88.46	174.81	−0.26761	0	9.996388
20	−87.88	188.23	−0.63369	0	19.98954
30	−87.01	177.91	−1.15493	0	29.97593
40	−87.30	185.53	−1.62376	0	39.96483
50	−87.11	180.02	−2.12792	0	49.95212
60	−86.57	186.05	−2.72457	−0.11844	59.93410
70	−86.46	180.11	−3.34199	−0.11963	69.91503
80	−87.18	181.58	−3.83375	−0.13320	79.90292
90	−87.03	181.14	−4.35174	−0.14351	89.88949
95	−87.90	189.88	−4.53223	−0.17495	94.88613

Borehole 2

Station (m)	Dip (degrees)	Azimuth (degrees)	x (m)	y (m)	z (m)
10	−41.95	32.21	6.292673	3.964254	6.684832
20	−44.18	37.89	11.95237	8.368637	13.65399
30	−43.44	47.76	16.83344	13.74418	20.52995
40	−45.62	38.01	22.34413	18.05116	27.67713
50	−47.73	36.33	27.7629	22.03603	35.07698
60	−51.02	32.61	33.06173	25.42608	42.85065
70	−52.95	42.09	37.53291	29.46470	50.83177
80	−56.14	33.84	42.16069	32.56741	59.13579
90	−54.13	40.90	46.58958	36.40385	67.23929
100	−56.24	37.41	51.00365	39.77990	75.55303
110	−55.77	49.18	54.68071	44.03683	83.82090
120	−54.63	47.04	58.62551	48.27305	91.97522
130	−56.21	47.70	62.36846	52.38651	100.2861
140	−53.30	45.46	66.56022	56.64614	108.3038
150	−55.97	48.96	70.23463	60.86713	116.5913
160	−56.38	45.35	74.12643	64.80541	124.9186
170	−55.02	44.11	78.24266	68.79573	133.1121
180	−54.65	47.63	82.14171	73.07024	141.2685

Borehole 3

Station (m)	Dip (degrees)	Azimuth (degrees)	x (m)	y (m)	z (m)
10	−39.54	84.91	0.684165	7.681386	6.366181
20	−41.62	88.35	0.899393	15.15394	13.00806
30	−41.24	89.53	0.961049	22.67322	19.60022
40	−41.12	71.54	3.346400	29.81893	26.17662
50	−40.57	93.84	2.837658	37.39798	32.68040
60	−40.77	85.21	3.470038	44.94490	39.21065
70	−41.56	94.51	2.881630	52.40433	45.84471
80	−41.13	90.17	2.859255	59.93648	52.42242
90	−42.15	86.88	3.262748	67.33939	59.13317
100	−43.11	88.37	3.470382	74.63685	65.96719
110	−44.49	92.12	3.206462	81.76568	72.97505
120	−43.58	98.16	2.178217	88.93645	79.86873
125	−43.69	100.69	1.507558	92.48912	83.32252

Borehole 4

Station (m)	Dip (degrees)	Azimuth (degrees)	x (m)	y (m)	z (m)
20	−89.33	25.49	0.211039	0.100615	19.99863
30	−87.92	59.41	0.395722	0.413024	29.99205
40	−87.55	83.95	0.440771	0.838083	39.98291
50	−85.17	82.74	0.547169	1.673295	49.94741
60	−85.43	85.45	0.610371	2.467520	59.91562
70	−85.47	80.93	0.734869	3.247423	69.88438
80	−82.89	81.22	0.923791	4.470633	79.80749
90	−82.43	79.95	1.153673	5.767761	89.72034

Appendix 2

BIPS mapped structures in the boreholes

Bh	Recorded Length	m.a.s.l.	Width	Strike	Dip	Weight	Sort	Form	Condition	Remark
Bh1	6.60	4.91	3	282	22	1.08	Fracture	Undulating	Cavities	Chlorite
Bh1	8.22	3.29	0	67	46	1.44	Structure	Foliation	Dull	Granite
Bh1	10.14	1.36	2	188	22	1.08	Fracture	Undulating	Cavities	Chlorite
Bh1	13.01	−1.50	8	23	76	4.13	Fracture	Irregular	Dull	Chlorite
Bh1	13.14	−1.63	8	359	81	5.00	Fracture	Irregular	Cavities	Chlorite
Bh1	13.49	−1.98	9	332	80	5.00	Fracture	Irregular	Cavities	Chlorite
Bh1	13.97	−2.46	23	94	35	1.22	Vein	Undulating	Dull	Pegmatite
Bh1	14.41	−2.89	412	72	80	5.00	Vein	Undulating	Dull	Fine grained
Bh1	15.44	−3.92	6	13	79	5.00	Fracture	Irregular	Dull	Chlorite
Bh1	20.85	−9.33	37	96	42	1.35	Vein	Undulating	Dull	Granite
Bh1	23.27	−11.75	0	49	52	1.62	Structure	Foliation	Dull	Granite
Bh1	33.82	−22.29	1	330	9	1.01	Fracture	Undulating	Weathered	Chlorite
Bh1	33.87	−22.34	1	357	10	1.02	Fracture	Undulating	Weathered	Chlorite
Bh1	34.08	−22.55	3	64	10	1.02	Fracture	Undulating	Cavities	Chlorite
Bh1	37.69	−26.16	24	136	29	1.14	Fracture	Undulating	Cavities	Chlorite
Bh1	38.96	−27.42	2	81	6	1.01	Fracture	Undulating	Cavities	Chlorite
Bh1	39.19	−27.66	1	136	16	1.04	Fracture	Undulating	Cavities	Calcite
Bh1	41.38	−29.84	2	153	7	1.01	Fracture	Undulating	Cavities	Chlorite
Bh1	45.52	−33.98	1	45	10	1.02	Fracture	Planar	Cavities	Chlorite
Bh1	46.20	−34.66	4	109	40	1.31	Fracture	Undulating	Cavities	Chlorite
Bh1	49.52	−37.97	1	116	6	1.01	Fracture	Undulating	Dull	Chlorite
Bh1	53.56	−42.01	5	76	22	1.08	Fracture	Undulating	Cavities	Chlorite
Bh1	55.09	−43.54	2	141	9	1.01	Fracture	Undulating	Weathered	Chlorite
Bh1	55.87	−44.32	4	345	81	5.00	Fracture	Irregular	Dull	Chlorite
Bh1	55.90	−44.35	3	138	13	1.03	Fracture	Undulating	Weathered	Chlorite
Bh1	58.91	−47.35	9	136	23	1.09	Vein	Undulating	Dull	Pegmatite
Bh1	60.43	−48.87	6	5	83	5.00	Fracture	Irregular	Dull	Chlorite
Bh1	60.88	−49.32	3	83	28	1.13	Fracture	Undulating	Cavities	Chlorite
Bh1	62.08	−50.53	10	114	55	1.74	Vein	Irregular	Dull	Pegmatite
Bh1	64.63	−53.07	0	108	40	1.31	Structure	Foliation	Dull	Granite
Bh1	65.04	−53.48	4	78	49	1.52	Fracture	Undulating	Weathered	Chlorite
Bh1	67.59	−56.03	10	324	78	5.00	Fracture	Undulating	Dull	Chlorite
Bh1	68.38	−56.82	15	356	79	5.00	Fracture	Undulating	Dull	Chlorite
Bh1	69.65	−58.09	0	72	20	1.06	Fracture	Undulating	Cavities	Chlorite
Bh1	75.45	−63.88	1	86	26	1.11	Fracture	Undulating	Weathered	Chlorite
Bh1	75.99	−64.42	1	75	31	1.17	Fracture	Undulating	Cavities	Chlorite
Bh1	76.05	−64.49	14	143	76	4.13	Fracture	Irregular	Dull	Chlorite
Bh1	76.80	−65.23	7	76	36	1.24	Fracture	Undulating	Weathered	Chlorite
Bh1	77.08	−65.51	7	69	44	1.39	Fracture	Undulating	Weathered	Chlorite
Bh1	78.13	−66.56	2	256	2	1.00	Fracture	Undulating	Weathered	Chlorite

Bh	Recorded Length	m.a.s.l.	Width	Strike	Dip	Weight	Sort	Form	Condition	Remark
Bh1	78.44	−66.87	1	238	30	1.15	Fracture	Undulating	Dull	Chlorite
Bh1	79.09	−67.52	9	167	86	5.00	Fracture	Irregular	Weathered	Chlorite
Bh1	79.32	−67.75	6	228	60	2.00	Fracture	Undulating	Open	Chlorite
Bh1	79.41	−67.84	1	276	9	1.01	Fracture	Undulating	Dull	Chlorite
Bh1	80.11	−68.53	10	155	40	1.31	Fracture	Irregular	Open	Chlorite
Bh1	81.15	−69.58	22	223	32	1.18	Fracture	Undulating	Open	Chlorite
Bh1	81.95	−70.37	10	179	84	5.00	Fracture	Irregular	Dull	Chlorite
Bh1	84.32	−72.75	2	69	21	1.07	Fracture	Undulating	Weathered	Chlorite
Bh1	84.36	−72.79	1	80	25	1.10	Fracture	Undulating	Cavities	Chlorite
Bh1	84.54	−72.97	154	244	25	1.10	Vein	Undulating	Dull	Pegmatite
Bh1	84.76	−73.18	30	83	15	1.04	Fracture	Irregular	Open	Chlorite
Bh1	85.12	−73.55	225	198	76	4.13	Vein	Undulating	Dull	Pegmatite
Bh1	85.17	−73.59	0	260	7	1.01	Fracture	Undulating	Weathered	Chlorite
Bh1	85.24	−73.67	2	171	2	1.00	Fracture	Undulating	Weathered	Chlorite
Bh1	86.51	−74.93	0	163	43	1.37	Structure	Foliation	Dull	Granite
Bh1	91.46	−79.88	119	68	49	1.52	Vein	Undulating	Dull	Pegmatite
Bh1	93.42	−81.84	34	88	44	1.39	Vein	Undulating	Dull	Pegmatite
Bh1	94.04	−82.46	17	47	63	2.20	Vein	Undulating	Dull	Pegmatite
Bh2	8.84	4.71	16	1	82	5.00	Fracture	Undulating	Weathered	Chlorite
Bh2	9.24	4.40	35	334	13	1.03	Fracture	Undulating	Open	Chlorite
Bh2	9.57	4.15	8	148	10	1.02	Fracture	Undulating	Weathered	Chlorite
Bh2	9.68	4.06	16	109	17	1.05	Fracture	Undulating	Open	Chlorite
Bh2	12.73	1.72	8	247	18	1.05	Fracture	Undulating	Open	Chlorite
Bh2	14.54	0.33	12	187	80	5.00	Fracture	Undulating	Cavities	Chlorite
Bh2	18.63	−2.81	52	117	37	1.25	Vein	Undulating	Dull	Fine grained
Bh2	19.86	−3.76	196	92	51	1.59	Vein	Undulating	Dull	Fine grained
Bh2	21.45	−4.98	0	124	25	1.10	Structure	Foliation	Dull	Granite
Bh2	22.62	−5.88	45	323	87	5.00	Vein	Undulating	Dull	Fine grained
Bh2	24.02	−6.96	41	275	73	3.42	Vein	Undulating	Dull	Fine grained
Bh2	25.52	−8.11	60	96	87	5.00	Vein	Undulating	Dull	Fine grained
Bh2	26.34	−8.73	253	88	86	5.00	Vein	Irregular	Dull	Fine grained
Bh2	27.86	−9.90	0	98	77	5.00	Structure	Foliation	Dull	Granite
Bh2	29.51	−11.17	16	15	89	5.00	Fracture	Undulating	Weathered	Chlorite
Bh2	31.05	−12.36	111	288	85	5.00	Vein	Undulating	Dull	Pegmatite
Bh2	33.78	−14.45	0	140	17	1.05	Structure	Foliation	Dull	Granite
Bh2	34.09	−14.69	167	146	70	2.92	Vein	Irregular	Dull	Pegmatite
Bh2	34.62	−15.10	66	95	70	2.92	Vein	Irregular	Dull	Fine grained
Bh2	34.85	−15.27	0	300	82	5.00	Structure	Foliation	Dull	Granite
Bh2	36.40	−16.46	129	100	84	5.00	Vein	Undulating	Dull	Fine.gran
Bh2	36.91	−16.86	0	87	63	2.20	Structure	Foliation	Dull	Granite
Bh2	37.85	−17.58	29	95	82	5.00	Vein	Undulating	Dull	Fine grained
Bh2	39.24	−18.65	129	105	76	4.13	Vein	Undulating	Dull	Fine grained
Bh2	54.63	−30.47	430	102	60	2.00	Vein	Irregular	Dull	Granite
Bh2	56.12	−31.62	114	96	80	5.00	Vein	Undulating	Dull	Fine grained
Bh2	57.68	−32.82	5	344	87	5.00	Fracture	Undulating	Cavities	Chlorite
Bh2	59.09	−33.90	857	304	13	1.03	Vein	Irregular	Dull	Granite
Bh2	66.28	−39.42	13	338	88	5.00	Fracture	Undulating	Weathered	Chlorite

Bh	Recorded Length	m.a.s.l.	Width	Strike	Dip	Weight	Sort	Form	Condition	Remark
Bh2	67.34	−40.23	40	90	67	2.56	Vein	Undulating	Dull	Chlorite
Bh2	68.44	−41.08	38	89	77	5.00	Vein	Undulating	Dull	Fine grained
Bh2	68.75	−41.32	4	168	89	5.00	Fracture	Undulating	Weathered	Chlorite
Bh2	68.98	−41.50	5	95	59	1.94	Fracture	Undulating	Cavities	Chlorite
Bh2	71.87	−43.71	8	321	28	1.13	Fracture	Planar	Open	Chlorite
Bh2	73.19	−44.73	2	333	84	5.00	Fracture	Undulating	Cavities	Chlorite
Bh2	74.51	−45.75	5	177	83	5.00	Fracture	Undulating	Cavities	Chlorite
Bh2	79.36	−49.47	241	97	76	4.13	Vein	Undulating	Dull	Fine grained
Bh2	81.53	−51.14	15	89	77	5.00	Vein	Undulating	Dull	Fine grained
Bh2	81.77	−51.32	51	102	60	2.00	Vein	Undulating	Dull	Fine grained
Bh2	82.47	−51.86	4	63	29	1.14	Fracture	Undulating	Weathered	Chlorite
Bh2	82.59	−51.95	3	33	24	1.09	Fracture	Undulating	Weathered	Chlorite
Bh2	82.79	−52.10	5	15	23	1.09	Fracture	Undulating	Weathered	Chlorite
Bh2	83.40	−52.57	59	119	46	1.44	Vein	Undulating	Dull	Fine grained
Bh2	83.72	−52.82	11	70	81	5.00	Fracture	Undulating	Weathered	Chlorite
Bh2	84.09	−53.10	8	0	26	1.11	Fracture	Undulating	Cavities	Chlorite
Bh2	89.66	−57.39	21	90	70	2.92	Vein	Undulating	Dull	Fine grained
Bh2	90.74	−58.21	202	90	69	2.79	Vein	Undulating	Dull	Fine grained
Bh2	92.12	−59.28	14	298	75	3.86	Fracture	Undulating	Weathered	Chlorite
Bh2	92.43	−59.51	38	82	78	5.00	Vein	Irregular	Dull	Chlorite
Bh2	93.32	−60.20	2	97	32	1.18	Fracture	Undulating	Cavities	Chlorite
Bh2	97.77	−63.61	53	105	71	3.07	Vein	Undulating	Dull	Fine grained
Bh2	97.92	−63.73	132	98	67	2.56	Vein	Undulating	Dull	Fine grained
Bh2	98.01	−63.80	3	157	75	3.86	Fracture	Undulating	Oxidized	Calcite
Bh2	100.77	−65.92	62	91	77	5.00	Vein	Undulating	Dull	Fine grained
Bh2	101.94	−66.82	50	73	65	2.37	Vein	Undulating	Dull	Fine grained
Bh2	103.86	−68.29	30	72	76	4.13	Vein	Undulating	Dull	Fine grained
Bh2	104.29	−68.62	12	339	87	5.00	Fracture	Undulating	Cavities	Chlorite
Bh2	104.74	−68.97	3	78	18	1.05	Fracture	Undulating	Weathered	Chlorite
Bh2	104.95	−69.13	9	143	72	3.24	Fracture	Undulating	Cavities	Chlorite
Bh2	105.51	−69.56	3	130	89	5.00	Fracture	Undulating	Cavities	Chlorite
Bh2	105.92	−69.87	2	131	85	5.00	Fracture	Undulating	Cavities	Chlorite
Bh2	106.12	−70.03	22	89	70	2.92	Vein	Undulating	Dull	Pegmatite
Bh2	106.72	−70.49	65	71	69	2.79	Vein	Irregular	Dull	Chlorite
Bh2	106.86	−70.60	55	89	54	1.70	Vein	Undulating	Dull	Pegmatite
Bh2	107.59	−71.16	10	316	81	5.00	Fracture	Undulating	Weathered	Chlorite
Bh2	108.13	−71.57	9	161	86	5.00	Fracture	Irregular	Weathered	Chlorite
Bh2	108.50	−71.86	3	80	41	1.33	Fracture	Undulating	Cavities	Chlorite
Bh2	108.53	−71.88	4	71	34	1.21	Fracture	Undulating	Cavities	Chlorite
Bh2	108.87	−72.14	8	73	59	1.94	Fracture	Undulating	Cavities	Chlorite
Bh2	109.62	−72.72	10	79	76	4.13	Vein	Undulating	Dull	Fine grained
Bh2	109.97	−72.98	251	65	81	5.00	Vein	Undulating	Dull	Fine grained
Bh2	111.01	−73.78	16	87	57	1.84	Vein	Undulating	Dull	Pegmatite
Bh2	113.88	−75.99	3	173	89	5.00	Fracture	Undulating	Cavities	Calcite
Bh2	116.82	−78.25	30	94	80	5.00	Vein	Undulating	Dull	Chlorite
Bh2	118.35	−79.42	7	53	34	1.21	Fracture	Undulating	Open	Chlorite
Bh2	118.93	−79.87	10	174	87	5.00	Fracture	Undulating	Weathered	Chlorite

Bh	Recorded Length	m.a.s.l.	Width	Strike	Dip	Weight	Sort	Form	Condition	Remark
Bh2	121.58	−81.91	82	91	81	5.00	Vein	Undulating	Dull	Fine grained
Bh2	122.96	−82.97	5	338	74	3.63	Fracture	Undulating	Weathered	Chlorite
Bh2	123.40	−83.31	88	99	72	3.24	Vein	Undulating	Dull	Fine grained
Bh2	124.53	−84.18	5	84	25	1.10	Fracture	Undulating	Weathered	Chlorite
Bh2	124.64	−84.26	3	92	24	1.09	Fracture	Undulating	Cavities	Chlorite
Bh2	125.10	−84.62	5	62	46	1.44	Fracture	Undulating	Cavities	Chlorite
Bh2	126.22	−85.47	7	336	88	5.00	Fracture	Undulating	Weathered	Chlorite
Bh2	127.69	−86.60	4	82	24	1.09	Fracture	Undulating	Weathered	Chlorite
Bh2	127.99	−86.83	3	108	50	1.56	Fracture	Undulating	Cavities	Chlorite
Bh2	128.22	−87.01	6	156	77	5.00	Fracture	Undulating	Cavities	Chlorite
Bh2	128.68	−87.36	2	146	86	5.00	Fracture	Undulating	Weathered	Chlorite
Bh2	128.81	−87.46	19	90	75	3.86	Vein	Undulating	Dull	Fine grained
Bh2	129.20	−87.76	7	142	88	5.00	Fracture	Undulating	Weathered	Chlorite
Bh2	130.48	−88.74	6	178	87	5.00	Fracture	Undulating	Weathered	Chlorite
Bh2	131.32	−89.39	7	257	22	1.08	Fracture	Undulating	Weathered	Chlorite
Bh2	131.49	−89.52	5	189	76	4.13	Fracture	Undulating	Weathered	Chlorite
Bh2	132.06	−89.96	10	194	81	5.00	Fracture	Undulating	Weathered	Chlorite
Bh2	133.72	−91.23	133	98	69	2.79	Vein	Undulating	Dull	Pegmatite
Bh2	134.29	−91.68	6	181	88	5.00	Fracture	Undulating	Weathered	Chlorite
Bh2	135.12	−92.31	9	184	86	5.00	Fracture	Undulating	Cavities	Chlorite
Bh2	135.89	−92.90	6	176	87	5.00	Fracture	Undulating	Weathered	Chlorite
Bh2	137.47	−94.12	8	295	38	1.27	Fracture	Undulating	Cavities	Chlorite
Bh2	138.33	−94.78	12	104	62	2.13	Vein	Irregular	Dull	Chlorite
Bh2	138.60	−94.98	74	92	76	4.13	Vein	Undulating	Dull	Pegmatite
Bh2	138.92	−95.23	17	93	63	2.20	Vein	Undulating	Dull	Fine grained
Bh2	139.44	−95.63	13	235	37	1.25	Fracture	Undulating	Open	Chlorite
Bh2	139.68	−95.81	6	344	87	5.00	Fracture	Undulating	Weathered	Chlorite
Bh2	141.91	−97.53	6	141	85	5.00	Fracture	Undulating	Weathered	Chlorite
Bh2	144.72	−99.68	8	238	14	1.03	Fracture	Undulating	Weathered	Chlorite
Bh2	145.97	−100.64	7	335	85	5.00	Fracture	Undulating	Cavities	Chlorite
Bh2	146.59	−101.12	49	112	81	5.00	Vein	Undulating	Dull	Fine grained
Bh2	147.93	−102.15	10	283	37	1.25	Fracture	Undulating	Cavities	Chlorite
Bh2	150.25	−103.94	1	304	87	5.00	Fracture	Undulating	Weathered	Chlorite
Bh2	152.83	−105.92	16	174	13	1.03	Fracture	Irregular	Open	Chlorite
Bh2	153.37	−106.33	6	155	87	5.00	Fracture	Undulating	Cavities	Chlorite
Bh2	153.53	−106.46	6	217	6	1.01	Fracture	Undulating	Weathered	Chlorite
Bh2	154.92	−107.53	3	314	81	5.00	Fracture	Undulating	Weathered	Chlorite
Bh2	156.33	−108.60	5	267	27	1.12	Fracture	Undulating	Weathered	Chlorite
Bh2	159.00	−110.66	2	337	87	5.00	Fracture	Undulating	Weathered	Chlorite
Bh2	160.17	−111.56	4	328	82	5.00	Fracture	Undulating	Weathered	Chlorite
Bh2	160.24	−111.61	3	270	8	1.01	Fracture	Undulating	Weathered	Chlorite
Bh3	6.99	9.88	26	203	74	3.63	Vein	Planar	Dull	Quartz
Bh3	11.01	7.23	12	60	13	1.03	Fracture	Planar	Cavities	Chlorite
Bh3	13.12	5.84	3	167	13	1.03	Fracture	Planar	Cavities	Chlorite
Bh3	14.37	5.01	18	208	74	3.63	Vein	Planar	Dull	Pegmatite
Bh3	15.31	4.39	0	153	70	2.92	Structure	Foliation	Dull	Granite
Bh3	16.52	3.60	12	65	84	5.00	Fracture	Planar	Dull	Chlorite

Bh	Recorded Length	m.a.s.l.	Width	Strike	Dip	Weight	Sort	Form	Condition	Remark
Bh3	17.84	2.73	23	144	45	1.41	Vein	Undulating	Dull	Pegmatite
Bh3	18.15	2.52	0	200	18	1.05	Structure	Foliation	Dull	Granite
Bh3	19.13	1.88	38	145	56	1.79	Vein	Undulating	Dull	Pegmatite
Bh3	20.26	1.13	14	31	22	1.08	Fracture	Undulating	Dull	Chlorite
Bh3	23.13	−0.77	395	105	64	2.28	Vein	Undulating	Dull	Fine grained
Bh3	24.67	−1.78	30	113	63	2.20	Vein	Undulating	Dull	Pegmatite
Bh3	24.92	−1.95	0	144	12	1.02	Structure	Foliation	Dull	Granite
Bh3	26.43	−2.94	4	333	85	5.00	Fracture	Irregular	Weathered	Chlorite
Bh3	28.79	−4.50	101	195	83	5.00	Vein	Undulating	Ep-sized	Epidote
Bh3	32.73	−7.10	16	259	81	5.00	Fracture	Irregular	Dull	Chlorite
Bh3	33.97	−7.92	1	193	71	3.07	Fracture	Undulating	Dull	Chlorite
Bh3	34.15	−8.04	0	191	28	1.13	Structure	Foliation	Dull	Granite
Bh3	34.83	−8.49	3	178	89	5.00	Fracture	Undulating	Ep-sized	Chlorite
Bh3	35.82	−9.14	2	207	67	2.56	Fracture	Undulating	Oxidized	Chlorite
Bh3	37.68	−10.37	2	208	72	3.24	Fracture	Planar	Weathered	Chlorite
Bh3	42.09	−13.28	4	206	72	3.24	Fracture	Planar	Weathered	Chlorite
Bh3	43.73	−14.36	6	57	10	1.02	Fracture	Undulating	Weathered	Chlorite
Bh3	44.67	−14.98	85	101	70	2.92	Vein	Undulating	Dull	Fine grained
Bh3	46.16	−15.97	3	96	53	1.66	Fracture	Undulating	Dull	Chlorite
Bh3	46.63	−16.28	18	115	56	1.79	Vein	Undulating	Dull	Pegmatite
Bh3	47.56	−16.89	1	164	74	3.63	Fracture	Planar	Cavities	Calcite
Bh3	50.33	−18.72	54	157	55	1.74	Vein	Undulating	Dull	Fine grained
Bh3	51.22	−19.30	6	233	85	5.00	Fracture	Undulating	Weathered	Chlorite
Bh3	52.62	−20.23	6	351	19	1.06	Fracture	Irregular	Weathered	Chlorite
Bh3	54.88	−21.72	1	191	66	2.46	Fracture	Planar	Cavities	Chlorite
Bh3	55.48	−22.12	6	89	17	1.05	Fracture	Irregular	Weathered	Chlorite
Bh3	56.46	−22.77	15	107	85	5.00	Vein	Irregular	Dull	Fine grained
Bh3	58.36	−24.02	87	188	73	3.42	Vein	Undulating	Dull	Pegmatite
Bh3	60.06	−25.14	12	103	73	3.42	Vein	Undulating	Dull	Fine grained
Bh3	62.33	−26.63	5	6	7	1.01	Fracture	Undulating	Weathered	Chlorite
Bh3	63.26	−27.25	2	165	69	2.79	Fracture	Undulating	Cavities	Chlorite
Bh3	65.60	−28.79	20	98	75	3.86	Vein	Planar	Dull	Fine grained
Bh3	66.30	−29.26	2	343	86	5.00	Fracture	Planar	Weathered	Chlorite
Bh3	66.72	−29.53	296	92	72	3.24	Vein	Undulating	Dull	Fine grained
Bh3	67.67	−30.16	6	170	87	5.00	Fracture	Undulating	Dull	Chlorite
Bh3	68.76	−30.88	18	112	50	1.56	Vein	Undulating	Dull	Pegmatite
Bh3	70.93	−32.31	8	153	8	1.01	Fracture	Undulating	Dull	Chlorite
Bh3	72.06	−33.06	2	186	88	5.00	Fracture	Undulating	Dull	Chlorite
Bh3	72.53	−33.37	46	28	19	1.06	Fracture	Planar	Open	Calcite
Bh3	74.65	−34.77	9	183	87	5.00	Fracture	Undulating	Dull	Chlorite
Bh3	74.82	−34.88	20	52	11	1.02	Fracture	Undulating	Dull	Chlorite
Bh3	75.96	−35.63	8	173	69	2.79	Fracture	Undulating	Dull	Chlorite
Bh3	76.28	−35.85	10	150	76	4.13	Fracture	Undulating	Dull	Chlorite
Bh3	76.84	−36.21	10	6	16	1.04	Fracture	Undulating	Dull	Chlorite
Bh3	78.35	−37.21	17	10	89	5.00	Fracture	Undulating	Dull	Chlorite
Bh3	79.42	−37.92	161	120	58	1.89	Vein	Undulating	Dull	Fine grained
Bh3	81.59	−39.35	31	174	87	5.00	Fracture	Undulating	Open	Chlorite

Bh	Recorded Length	m.a.s.l.	Width	Strike	Dip	Weight	Sort	Form	Condition	Remark
Bh3	85.51	−41.93	23	5	89	5.00	Fracture	Undulating	Dull	Chlorite
Bh3	89.17	−44.35	22	59	35	1.22	Vein	Undulating	Dull	Fine grained
Bh3	103.30	−53.68	22	254	84	5.00	Vein	Undulating	Dull	Fine grained
Bh3	103.92	−54.09	1	178	43	1.37	Fracture	Planar	Cavities	Calcite
Bh3	108.83	−57.33	129	189	88	5.00	Vein	Undulating	Dull	Pegmatite
Bh3	110.92	−58.71	97	185	76	4.13	Vein	Undulating	Dull	Pegmatite
Bh4	14.91	−1.37	0	116	27	1.12	Structure	Foliation	Dull	Granite
Bh4	15.49	−1.95	2	35	16	1.04	Fracture	Undulating	Cavities	Chlorite
Bh4	15.68	−2.13	2	228	26	1.11	Fracture	Planar	Dull	Chlorite
Bh4	18.16	−4.61	1	245	32	1.18	Fracture	Planar	Dull	Chlorite
Bh4	19.64	−6.08	2	342	6	1.01	Fracture	Planar	Cavities	Chlorite
Bh4	20.63	−7.07	2	252	24	1.09	Fracture	Planar	Cavities	Chlorite
Bh4	21.30	−7.74	2	222	19	1.06	Fracture	Planar	Cavities	Chlorite
Bh4	21.33	−7.77	1	235	22	1.08	Fracture	Planar	Cavities	Chlorite
Bh4	22.15	−8.58	4	278	45	1.41	Fracture	Planar	Cavities	Chlorite
Bh4	25.13	−11.56	117	115	82	5.00	Vein	Undulating	Dull	Pegmatite
Bh4	26.34	−12.77	38	82	73	3.42	Vein	Irregular	Dull	Pegmatite
Bh4	27.32	−13.74	6	166	72	3.24	Fracture	Irregular	Weathered	Chlorite
Bh4	28.59	−15.01	3	305	41	1.33	Fracture	Planar	Cavities	Chlorite
Bh4	29.47	−15.88	32	72	79	5.00	Vein	Undulating	Dull	Pegmatite
Bh4	35.65	−22.04	10	100	73	3.42	Vein	Undulating	Dull	Pegmatite
Bh4	36.91	−23.31	0	147	42	1.35	Structure	Foliation	Dull	Granite
Bh4	37.17	−23.56	1	68	9	1.01	Fracture	Planar	Weathered	Chlorite
Bh4	37.21	−23.60	2	49	7	1.01	Fracture	Planar	Weathered	Chlorite
Bh4	37.38	−23.77	87	94	69	2.79	Vein	Undulating	Dull	Fine grained
Bh4	38.46	−24.85	2	32	4	1.00	Fracture	Planar	Weathered	Chlorite
Bh4	39.22	−25.61	9	67	78	5.00	Vein	Undulating	Dull	Fine grained
Bh4	39.67	−26.06	153	70	73	3.42	Vein	Undulating	Dull	Fine grained
Bh4	41.24	−27.62	44	97	62	2.13	Vein	Undulating	Dull	Fine grained
Bh4	41.59	−27.97	183	94	73	3.42	Vein	Undulating	Dull	Fine grained
Bh4	42.42	−28.80	2	267	21	1.07	Fracture	Undulating	Dull	Calcite
Bh4	42.91	−29.29	7	109	59	1.94	Vein	Undulating	Dull	Fine grained
Bh4	44.22	−30.60	4	308	10	1.02	Fracture	Undulating	Cavities	Chlorite
Bh4	45.47	−31.84	1	137	15	1.04	Fracture	Planar	Weathered	Chlorite
Bh4	45.70	−32.07	2	109	16	1.04	Fracture	Planar	Dull	Chlorite
Bh4	45.97	−32.34	274	119	44	1.39	Vein	Undulating	Dull	Fine grained
Bh4	46.57	−32.94	16	292	81	5.00	Fracture	Irregular	Weathered	Chlorite
Bh4	47.73	−34.10	1	272	13	1.03	Fracture	Undulating	Dull	Chlorite
Bh4	48.03	−34.39	2	263	13	1.03	Fracture	Undulating	Weathered	Chlorite
Bh4	48.36	−34.72	0	172	73	3.42	Contact	Planar	Dull	Pegmatite
Bh4	51.08	−37.44	0	80	58	1.89	Contact	Undulating	Dull	Granite
Bh4	51.75	−38.10	625	172	71	3.07	Vein	Undulating	Dull	Fine grained
Bh4	52.94	−39.29	2	128	18	1.05	Fracture	Undulating	Cavities	Chlorite
Bh4	53.24	−39.59	141	102	73	3.42	Vein	Undulating	Dull	Fine grained
Bh4	54.28	−40.63	286	90	75	3.86	Vein	Undulating	Dull	Fine grained
Bh4	55.08	−41.43	106	97	25	1.10	Vein	Planar	Oxidized	Pegmatite
Bh4	55.32	−41.66	133	43	26	1.11	Fracture	Undulating	Open	Chlorite

Bh	Recorded Length	m.a.s.l.	Width	Strike	Dip	Weight	Sort	Form	Condition	Remark
Bh4	56.06	−42.41	1	334	16	1.04	Fracture	Undulating	Weathered	Chlorite
Bh4	56.46	−42.80	1	166	17	1.05	Fracture	Undulating	Weathered	Chlorite
Bh4	57.04	−43.38	88	96	67	2.56	Vein	Irregular	Dull	Fine grained
Bh4	57.70	−44.04	11	94	41	1.33	Fracture	Undulating	Weathered	Chlorite
Bh4	57.96	−44.30	0	128	24	1.09	Structure	Foliation	Dull	Granite
Bh4	58.66	−44.99	186	112	72	3.24	Vein	Irregular	Dull	Fine grained
Bh4	58.94	−45.27	191	110	68	2.67	Vein	Irregular	Dull	Fine grained
Bh4	59.57	−45.90	60	116	78	5.00	Vein	Undulating	Dull	Fine grained
Bh4	60.84	−47.17	9	182	35	1.22	Vein	Undulating	Dull	Pegmatite
Bh4	61.51	−47.83	21	233	45	1.41	Vein	Undulating	Dull	Pegmatite
Bh4	61.89	−48.21	0	220	38	1.27	Structure	Foliation	Dull	Granite
Bh4	62.11	−48.44	24	115	54	1.70	Vein	Undulating	Dull	Fine grained
Bh4	62.28	−48.60	1	80	25	1.10	Fracture	Undulating	Weathered	Chlorite
Bh4	63.05	−49.37	57	245	64	2.28	Vein	Irregular	Dull	Fine grained
Bh4	63.54	−49.86	31	247	48	1.49	Vein	Irregular	Dull	Fine grained
Bh4	64.73	−51.04	1	123	5	1.00	Fracture	Undulating	Weathered	Chlorite
Bh4	64.75	−51.07	1	141	9	1.01	Fracture	Undulating	Weathered	Chlorite
Bh4	64.99	−51.31	3	132	2	1.00	Fracture	Undulating	Weathered	Chlorite
Bh4	67.75	−54.06	2	304	38	1.27	Fracture	Undulating	Dull	Calcite
Bh4	69.00	−55.31	1	309	12	1.02	Fracture	Undulating	Dull	Calcite
Bh4	69.02	−55.32	6	93	35	1.22	Fracture	Planar	Weathered	Chlorite
Bh4	69.14	−55.44	55	106	70	2.92	Vein	Irregular	Dull	Fine grained
Bh4	69.74	−56.05	1	284	13	1.03	Fracture	Undulating	Dull	Calcite
Bh4	69.97	−56.27	3	86	39	1.29	Fracture	Undulating	Dull	Chlorite
Bh4	70.00	−56.30	2	115	18	1.05	Fracture	Undulating	Cavities	Calcite
Bh4	70.04	−56.34	6	285	8	1.01	Fracture	Undulating	Dull	Calcite
Bh4	70.09	−56.40	1	271	23	1.09	Fracture	Undulating	Dull	Chlorite
Bh4	71.80	−58.10	4	271	8	1.01	Fracture	Undulating	Weathered	Chlorite
Bh4	71.87	−58.17	3	248	9	1.01	Fracture	Undulating	Weathered	Chlorite
Bh4	74.27	−60.56	1	50	15	1.04	Fracture	Undulating	Weathered	Chlorite
Bh4	75.28	−61.57	3	359	10	1.02	Fracture	Planar	Dull	Chlorite
Bh4	77.48	−63.76	28	94	75	3.86	Vein	Undulating	Dull	Fine grained
Bh4	77.69	−63.97	140	105	79	5.00	Vein	Irregular	Dull	Fine grained
Bh4	78.14	−64.42	130	107	74	3.63	Vein	Irregular	Dull	Fine grained
Bh4	79.00	−65.27	30	117	69	2.79	Vein	Undulating	Dull	Fine grained
Bh4	79.67	−65.95	20	112	60	2.00	Vein	Undulating	Dull	Fine grained
Bh4	80.34	−66.62	33	113	82	5.00	Vein	Undulating	Dull	Fine grained
Bh4	80.71	−66.98	13	112	68	2.67	Vein	Undulating	Dull	Fine grained
Bh4	81.37	−67.64	39	104	82	5.00	Vein	Irregular	Dull	Pegmatite
Bh4	83.28	−69.54	113	128	39	1.29	Vein	Undulating	Dull	Pegmatite
Bh4	84.49	−70.75	28	77	33	1.19	Fracture	Irregular	Weathered	Chlorite
Bh4	84.99	−71.25	6	308	19	1.06	Fracture	Undulating	Weathered	Chlorite
Bh4	85.77	−72.03	87	104	71	3.07	Vein	Undulating	Dull	Pegmatite
Bh4	86.59	−72.84	184	113	73	3.42	Vein	Undulating	Dull	Pegmatite
Bh4	87.17	−73.42	24	101	65	2.37	Vein	Undulating	Dull	Pegmatite
Bh4	88.11	−74.36	591	93	71	3.07	Vein	Undulating	Dull	Pegmatite
Bh4	89.85	−76.10	89	109	70	2.92	Vein	Undulating	Dull	Pegmatite

ISSN 1404-0344

CM Digitaltryck AB, Bromma, 2001